System Identification of a Class of Wiener Systems with Hysteretic Nonlinearities

A. Radouane[*], F. Giri[**], F. Ikhouane[***], T. Ahmed-Ali[**], F.Z. Chaoui[*], A. Brouri[****]

[*] ENSET, University of Mohammed V, Rabat, Morocco

[**] University of Caen Basse-Normandie, GREYC Lab UMR CNRS, 14032 Caen, France

[***] Universitat Politècnica de Catalunya, Departament de Matemàtica Aplicada III, 08036, Barcelona, Spain

[****] ENSAM, University of My Ismail, Meknes, Morocco

Abstract. Existing works on Wiener system identification have essentially been focused on the case where the output nonlinearity is memoryless. When memory nonlinearities have been considered, the focus has been restricted to backlash like nonlinearities. In this paper, we are considering Wiener systems where the output nonlinearity is a general hysteresis operator captured by the well known Bouc-Wen model. The Wiener system identification problem is addressed by making use of steady-state property, obtained in periodic regime, referred to as hysteretic loop assumption (HLA). The complexity of this problem comes from the system nonlinearity as well as its unknown parameters that enter in a nonaffine way in the model. It is shown that the linear part of the system is accurately identified using a frequency method. Then, the nonlinear hysteretic subsystem is identified, on the basis of a parameterized representation, using a prediction-error approach.

1. INTRODUCTION

Standard Wiener model is constituted of a linear dynamic subsystem and a memoryless nonlinearity connected in series as shown by Fig. 1. It is formally established that a wide range of nonlinear dynamic systems can be well approximated with parallel Wiener models (e.g. Boyd and Chua, 1985). Therefore, the problem of Wiener system identification has received a great deal of interest, especially during the last decade, and several solutions are now available. In the case of fully parametric systems, the proposed identification approaches include deterministic methods (e.g. Vörös, 1997, 2010; Bruls *et al.*, 1999) as well as stochastic methods (e.g. Wigren, 1993, 1994; Westwick and Verhaegen, 1996; Vanbeylen *et al.*, 2009; Lovera *et al.*, 2000; Wills and Ljung, 2010; Vanbeylen and Pintelon, 2010; Wills *et al.*, 2011). The available identification methods for nonparametric Wiener systems include stochastic methods (e.g. Greblicki and Pawlak, 2008; Mzyk, 2010) and frequency methods (e.g. Crama and Schoukens, 2001, 2005; Bai, 2003; Giri *et al.*, 2009; Schoukens and Rolain, 2012). Identification methods have also been proposed for semiparametric Wiener systems, where only the linear part is parameterized (e.g. Hu and Chen, 2008; Bai and Reyland, 2009; Enqvist, 2010; Pelckmans, 2011). All existing identification methods rely on several assumptions on the system nonlinear part (invertible, odd), on the linear subsystem (finite impulse response (FIR), known structure), and on input signals (Gaussian, persistently exciting (PE)). In recent years, the research scope concerning Wiener system identification has been extended to nonstandard Wiener system structures including series-parallel

Wiener systems (Lyzell and Enqvist, 2012; Lyzell et al., 2012; Schoukens and Rolain, 2012) and Wiener systems with memory nonlinearities (Dong *et al.*, 2009; Cerone *et al.*, 2009; Giri *et al.*, 2013, 2014; Reyland and Bai, 2013).

In the present study, we are interested in Wiener systems that contain memory nonlinearities. In (Dong *et al.*, 2009), the nonlinearity is a backlash operator bordered by two straight lines and a recursive least-squares method is used to get estimates of the linear subsystem parameters and the nonlinearity characteristics (e.g. border line slopes). In (Cerone *et al.*, 2009), the nonlinearity is also a backlash operator with straight line borders and a two-stage method is used to bound all system parameters. In (Giri *et al.*, 2013), the nonlinearity is a nonparametric backlash operator and the identification problem is dealt with using a frequency method based on analytic geometry tools. Nonparametric backlash operators are also considered in (Reyland and Bai, 2013) where it is established that the parameters of the linear FIR subsystem can be separately identified. In (Giri et al., 2014), the class of nonlinearities dealt with include backlash and backlash-inverse operators with polynomial borders and the identification method indifferently applies to both categories.

The above discussion shows that all existing works considering memory nonlinearities in Wiener system identification have been focused on backlash-like operators. Although the latter are more complex than memoryless nonlinearities, considered in earlier studies, their modelling capability is still not sufficient to capture all real-life memory components. One of their limitations lies in the fact that, the limit cycles spanned by their operating point (in steady-state periodic regimes) are laterally bordered by fixed functions independent on the input signal amplitude. Consequently, backlash-like models are unable to capture the more general hysteresis effect which leads to limit cycles (called hysteresis loops) whose border functions are depending on the input signal excursion. The hysteresis behaviour is encountered in several areas including biology, optics, electronics, ferroelectricity, magnetism, mechanics, structures, smart materials, and others. In mechanics and structures, hysteresis arises as a natural property of materials to supply restoring forces against movements and dissipate energy (Ikhouane and Rodellar, 2007). In recent years, the hysteresis effect has been deliberately introduced to design highly sophisticated equipments e.g. magnetorheological dampers (Aguirre et al., 2012), piezoelectrical actuators (Gomis-Bellmunt et al., 2009), micro- and nano-positionners (Kiong and Sunan, 2014), Li-ion batteries (Hu et al., 2012). Therefore, much interest has been paid to modelling and analyzing hysteresis phenomena, especially over the last three decades. Dozens of hysteresis models have thus been proposed including Duhem, Dahl, Colman-Hodgon, Prandtl, Preisach, Jiles-Atherton, Krasnoselski-Pokrovski, and others (Mayergoyz, 2003). The control of systems involving hysteresis effect is also a challenging problem that has received interest, see (Ikhouane and Rodellar, 2007; Kiong and Sunan, 2014) and references therein. The proposed control designs require the values of the parameters that represent the hysteresis effect. Clearly, system

identification constitutes a crucial part in such control designs because the parameters are generally unknown.

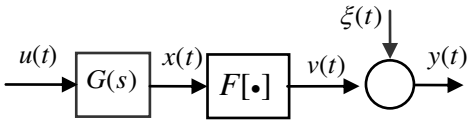

Fig. 1. Wiener model structure: $G(s)$ is a linear subsystem, $F[.]$ is a nonlinear operator.

In this paper, the problem of Wiener system identification is addressed in presence hysteresis output nonlinearities. As mentioned above, this problem has yet to be solved since earlier works on Wiener system identification have essentially been focused on memoryless nonlinearities and the few works that dealt with memory nonlinearities have been restricted to backlash type operators. Referring to Fig. 1, the output hysteretic operator, denoted $F[\bullet]$, may represent a sensor featuring hysteresis such as Hall effect sensors which are widely used by electrical engineers. Then, the complexity of the identification problem lies not only in the nonlinearity of the model dynamics, but also in its interconnected structure making its internal signals not accessible to measurements and its unknown parameters entering in the model nonlinearly. In this paper, we show that this complexity can be overcome if the hysteresis nonlinearity possesses the HLA property. Roughly, this property describes the steady-state behaviour of a hysteresis operator being excited by the so-called "loading-unloading" inputs (a class of periodic increasing-decreasing signals). HLA stipulates that the working point $(x(t), v(t))$ (see Fig. 1) spans a hysteresis loop, bordered by two strictly increasing lines only depending on the input excursion. Based on this property, the linear subsystem model is determined using a frequency identification approach. As long as the linear subsystem is concerned, no prior knowledge on the hysteresis subsystem is required at this first stage, except for the HLA property. The second stage of the identification method is devoted to parameter estimation of the hysteresis subsystem. Presently, this is illustrated considering the Bouc-Wen hysteresis model and parameter estimation is performed using nonlinear least-squares (LS) techniques. The developed identification method only involves periodic input signals. The required number of needed input signals depends on the properties of the linear subsystem and the available prior knowledge on it. In most favourable cases, two input signals are sufficient. The identification method enjoys the weak coupling between its two stages (which improves the accuracy of the estimated parameters) and the consistency of all involved estimators. The present paper is an extension of the authors' conference paper (Radouane et al., 2014) where the identification problem was dealt with for a reduced class of hysteresis systems. The latter were described by a simplified version of the Bouc-Wen model not involving the elastic term in the restoring force. Doing so, the identification problem becomes much simpler as it involves

less inaccessible signals and less non-affine parameters. Presently, a much wider class of hysteresis systems are accounted for making the problem much more complex.

The paper is organized as follows: the identification problem is formulated in Section 2; Section 3 is devoted to describing the linear subsystem identification and Section 4 to the hysteresis subsystem identification method; the performances of the identification method are illustrated by simulation in Section 5.

2. IDENTIFICATION PROBLEM FORMULATION

In this section, the Wiener system under study is analytically modelled, making use of the hysteresis loop assumption. Then, the identification objectives are described and the identifiability issue is discussed. Finally, a signal pre-processing method based on period averaging is introduced.

2.1 System Modelling

Standard Wiener systems consist of a linear dynamic subsystem $G(s)$ followed in series by a memoryless nonlinear element $F[\bullet]$, see Fig. 1. Presently, this element is allowed to be memory of hysteretic type. The overall Wiener system is analytically described by the following equations:

$$x = G(s)u \tag{1a}$$

$$v = F[x] \tag{1b}$$

$$y(t) = v(t) + \xi(t) \tag{1c}$$

where u and y denote the system input and output; x and v are internal signals not accessible to measurement. The signal ξ is a zero-mean ergodic noise featuring periodic stationarity, a property to be defined below (see Subsection 2.3). The transfer function $G(s)$ assumes no particular structure but it must be asymptotically stable to make possible open-loop system identification. Also, the element $F[\bullet]$ is any memory operator that is BIBO stable satisfying the hysteretic loop assumption (see hereafter). To describe this assumption, the following definition is needed (see e.g. Ikhouane and Rodellar, 2007):

Definition 1. A periodic signal z is said to be loading-unloading if it is continuous, periodic (with some period $T > 0$), and there exists a scalar $0 < \kappa < 1$ so that u is C^1 increasing on the interval $(0, \kappa T)$ and C^1 decreasing on the interval $(\kappa T, T)$.

Assumption HLA (Hysteretic Loop Assumption). Let the signal x in (1b) be loading-unloading, with $x_{\min} \le x(t) \le x_{\max}$ for some scalars $-\infty < x_{\min} < x_{\max} < \infty$. Then, the following properties hold with the resulting hysteresis output $v = F[x]$:

1) There exist two *strictly-increasing* C^1 functions V^+ and V^- such that, one has in steady-state:

$$v(t) = V^+(x(t)) \text{ for } t \in [mT, (m+\kappa)T), \quad m \in \mathbf{N} \tag{2a}$$

$$v(t) = V^-(x(t)) \text{ for } t \in [(m+\kappa)T, (m+1)T) \tag{2b}$$

$$V^+(x(mT)) = V^-(x(mT)) \text{ and } V^+\big(x((m+\kappa)T)\big) = V^-\big(x(m+\kappa)T)\big) \tag{2c}$$

where T and κ are as in Definition 1.

2) The functions (V^+, V^-) depend on the excursion interval $[x_{\min}, x_{\max}]$ of the signal x, but not on its period T. This property is commonly referred to as rate-independence.

3) Just as x, the signal v is T-periodic loading-unloading and the set $\{(x(t), v(t)); t \geq 0\}$ is an oriented closed locus referred to as (x, v)-hysteresis loop and (V^+, V^-) are its border functions.

Example 1. Consider the Bouc-Wen hysteresis model which is defined as follows:

$$v(t) = \lambda_x x(t) + \lambda_w w(t) \tag{3a}$$

$$\dot{w} = \alpha\dot{x} - \beta|\dot{x}||w|^{\mu-1}w - \gamma\dot{x}|w|^{\mu} \tag{3b}$$

with $\alpha > 0$, $\beta + \gamma > 0$, $\beta - \gamma \geq 0$, $\lambda_x > 0$, $\lambda_w > 0$ and $\mu > 1$, where w is an internal state variable. In the context of mechanical systems, $x(t)$ is a displacement and $v(t)$ a restoring force which appears as the superposition of an elastic component $\lambda_x x(t)$ and a purely hysteretic component $\lambda_w w(t)$. The parameters (α, β, γ) determine the shape and the size of the hysteresis loop, while the scalar μ determines the smoothness of the transition from elastic to plastic response. Clearly, equations (3a-b) entails a series-parallel structure of the Bouc-Wen hysteresis model, see also Fig. A1 in Appendix A. An extensive analysis can be found in chapters 2 and 3 of (Ikhouane and Rodellar, 2007) where it is formally shown that this hysteresis model is BIBO stable and satisfies Assumption HLA. Figs. 2a-b illustrate the hysteresis loops that can be generated by this model. Finally, note that the identification problem for the Wiener system (1a-c) in presence of a Bouc-Wen hysteresis, has already been considered in (Radouane et al., 2014) where an identification method has been designed. However, the study made there was limited to the case where $\lambda_x = 0$ and $\lambda_w = 1$ which entails the absence of elastic effect in the restoring force. In such a case, the model can only produce hysteresis loops centred on the origin which limits its practical applicability. On the other hand, the assumptions $\lambda_x = 0$ and $\lambda_w = 1$ makes the identification problem much simpler as the number of unknown parameters is smaller. Furthermore, these assumptions imply that $v(t) = x(t)$ leading to a reduced number of inaccessible signals. Moreover, the model structure boils down to a series interconnection, while it is a series-parallel in the general model (3a-b), see Fig. A1 in Appendix A. These model simplifications make the present identification problem much more complex compared to (Radouane et al., 2014).

2.2 System identification objective and identifiability issue.

The identification problem at hand is to accurately determine the two components of the system model i.e. the transfer function $G(s)$ and the hysteretic operator $F[\bullet]$. When $G(s)$ assumes no a priori

known structure, the identification purpose amounts to estimate its frequency response $G(j\omega)$, for a set of frequencies selected by the user. In case $G(s)$ assumes a known parameterized structure, the involved parameters must also be accurately estimated. A key feature of the presently proposed identification method is that the linear subsystem identification is coped with based only on Assumption HLA, i.e. the model structure of $F[\bullet]$ needs not to be a priori known. A parameterized model of $F[\bullet]$ is only needed in the second stage (of the identification method) which is devoted to the estimation of the hysteretic parameters. Presently, this stage will be illustrated in Section 4 considering the Bouc-Wen hysteresis model (3a-d).

As the internal signals (x, v) are inaccessible to measurements (see Fig. 1), system identification must only make use of the input and output signals (u, y). It turns out that the model $\big(G(s), F[\bullet]\big)$ is not uniquely determined by the Wiener model (1a-c). Indeed, any pair $\big(G^1(s), F^1[\bullet]\big)$, with $G^1(s) = kG(s)$ and $F^1[x] = F[x/k]$, is also a model, whatever the scalar $k \neq 0$. This identifiability issue is overcome by imposing additional constraints on the Wiener model. Simple constraints are: $\big|G^1(j\omega_1)\big| = \big|kG(j\omega_1)\big| = 1$ and $0 \leq \angle G^1(j\omega_1) < \pi$, with ω_1 any fixed frequency that is selected so that $\big|G(j\omega_1)\big| \neq 0$ (see Remark 1). Clearly, these constraints define a unique model corresponding to $|k| = 1/\big|G(j\omega_1)\big|$ and:

$$\mathrm{sgn}(k) = 1 \text{ if } \angle G(j\omega_1) \in [0, \pi) \quad \text{and} \quad \mathrm{sgn}(k) = -1 \text{ if } \angle G(j\omega_1) \in [\pi, 2\pi) \text{ (modulo } \pi).$$

Now, to avoid introducing additional notations, the particular model $(G^1(s), F^1[x])$ satisfying the above constraints will continue to be denoted $\big(G(s), F[x]\big)$ and the corresponding internal signals will still be denoted x and v. It turns out that the system model (1a-c) is completed with Assumption HLA and the following property:

$$\big|G(j\omega_1)\big| = 1 \text{ and } 0 \leq \angle G(j\omega_1) < \pi \quad \text{(modulo } \pi) \tag{4}$$

Remark 1. 1) Under conditions (4) and Assumption HLA, a consistent estimator of the frequency response $G(j\omega)$ will be designed in Section 3. This proves that (4) and HLA are sufficient conditions for frequency response identifiability. The identification of the hysteretic element $F[\bullet]$ will be dealt with in Section 4 based on the model (3a-b). There, an additional identifiability issue concerning only (3a-b) will be pointed out and coped with.

2) In (4), the frequency ω_1 is arbitrarily chosen by the user bearing in mind the condition $\big|G(j\omega_1)\big| \neq 0$. Now, let the sinusoidal input $u(t) = U_1 \cos(\omega_1 t)$ be applied to the Wiener system and let the resulting steady-state output of the linear subsystem be denoted $x_{U_1,\omega_1}(t) = U_1\big|G(j\omega_1)\big| \cos\big(\omega_1 t + \angle G(j\omega_1)\big)$. If $\big|G(j\omega_1)\big| \neq 0$ then x_{U_1,ω_1} is a nonzero loading-unloading signal. Therefore, by Assumption HLA the

hysteresis output, denoted $v_{U_1,\omega_1}(t)$, is also non-zero loading-unloading signal. On the other hand, if $|G(j\omega_1)|=0$ then the resulting (steady-state) internal signal x_{U_1,ω_1} will be zero leading to (a steady-state) constant signal v_{U_1,ω_1}. That is, the case $|G(j\omega_1)|=0$ can be easily detected by just monitoring v_{U_1,ω_1}. To get benefit of this result, one needs an accurate estimator of the (inaccessible) undisturbed output v_{U_1,ω_1} relying only on the system output y_{U_1,ω_1}. This is the subject of the next subsection.

2.3. Signal Pre-Processing

When system identification is performed in presence of periodic signals, with the same period T, the following T-periodic averaging process proves to be useful in coping with noise (Ljung, 1999, p.232):

$$\bar{z}_N(t)=\frac{1}{N}\sum_{k=0}^{N-1} z\big(t+kT\big),\ \text{for } 0\le t\le T \tag{5a}$$

$$\bar{z}_N(t)=\bar{z}_N(t-T),\ \text{otherwise} \tag{5b}$$

with $N>>1$, where z is any signal and $\bar{z}_N$ is referred to as its T-periodic average signal. It readily follows that $\bar{z}_N=z$ whenever z is itself T-periodic. In the present identification method, the signals (u,x,v) will be T-periodic and so all three are equal (in steady-state) to their T-periodic average versions obtained by (5a-b). Then, it follows from (1c) that (in steady-state):

$$\bar{y}_N(t)=v(t)+\bar{\xi}_N(t) \tag{6}$$

Accordingly, it is supposed that the noise $\xi(t)$ is zero-mean ergodic and features the T-periodic stationarity i.e.

$$E\big(\xi(t+kT)\big)=E(\xi(t))\text{; for all } t \text{ and } k\in\mathbf{N} \tag{7}$$

As $\xi(t)$ zero mean ergodic, one gets from (7):

$$\bar{\xi}_N(t)\underset{N\to\infty}{\to}E(\xi(t+kT))=0\quad\text{(w.p. 1)} \tag{8}$$

Then, it immediately follows from (6) that, in steady-state (i.e. when $v(t)$ becomes periodic):

$$\bar{y}_N(t)-v(t)\underset{N\to\infty}{\to}0\quad\text{(w.p. 1)} \tag{9}$$

3. LINEAR SUBSYSTEM PARAMETER IDENTIFICATION

In this section, it is shown that the linear subsystem $G(s)$ can be identified first. To this end, it is proved that, within specific operating conditions inspired by Assumption HLA, a (x,v)-hysteresis loop can be accurately estimated. Then, an accurate estimator of the linear subsystem output $x(t)$ is constructed and used to estimate $G(s)$.

3.1. Hysteresis Loop Estimation

By Assumption HLA, the hysteretic operator (1b) enjoys the rate-independence property. Accordingly, the (x,v)-hysteresis loop, generated by any loading-unloading signal $x(t)$, only depends on the

excursion interval $[x_{\min}, x_{\max}]$ of $x(t)$. All loading-unloading signals $x(t)$ with the same excursion interval lead to the same (x,v)-hysteresis loop, whatever their shapes and their frequencies. In this subsection, we aim at identifying the (x,v)-hysteresis loop that is obtained by all signals $x(t)$ spanning a given interval $[-U_1, U_1]$, where $U_1 > 0$ is arbitrarily chosen by the user. To this end, we make use of the data collected on the Wiener system (1a-c) being excited by the simple sinusoidal input $u_1(t) = U_1 \cos(\omega_1 t)$ where the frequency ω_1 is as in property (4), so that one gets benefit from that property. Doing so, the *steady-state* behaviour of the Wiener system (1a-c) turns out to be described by the following equalities:

$$x_{U_1,\omega_1}(t) = U_1 \cos\big(\omega_1 t + \angle G(j\omega_1)\big) \tag{10a}$$

$$v_{U_1,\omega_1} = F[x_{U_1,\omega_1}] \tag{10b}$$

$$y_{U_1,\omega_1}(t) = v_{U_1,\omega_1}(t) + \xi(t) \tag{10c}$$

where the index (U_1,ω_1) emphasizes the dependence (in steady-state) of all signals on the amplitude/frequency couple (U_1,ω_1). The most important feature of the linear subsystem output $x_{U_1,\omega_1}(t)$ is that it is loading-unloading and is spanning the interval $[-U_1, U_1]$. Then, by Assumption HLA, the resulting signal $v_{U_1,\omega_1}(t)$ is C^1 and $2\pi/\omega_1$-periodic loading-unloading, in steady-state. Furthermore, $v_{U_1,\omega_1}(t)$ is related to $x_{U_1,\omega_1}(t)$ by the hysteresis border functions. The latter are presently denoted $V_{U_1}^+$ and $V_{U_1}^-$ where the index U_1 emphasizes the fact that these functions only depend on the excursion interval $[-U_1, U_1]$ of the signal $x_{U_1,\omega_1}(t)$ (not on its frequency). By Assumption HLA, the relationship between the hysteresis input/output signals express as follows:

. On the half period $\left[\dfrac{2k\pi - \angle G(j\omega_1)}{\omega_1}, \dfrac{2k\pi - \angle G(j\omega_1) + \pi}{\omega_1}\right]$, where $\dot{x}_{U_1,\omega_1}(t) < 0$ and $\dot{v}_{U_1,\omega_1}(t) < 0$, one has:

$$v_{U_1,\omega_1}(t) = V_{U_1}^-(x_{U_1,\omega_1}(t)). \tag{11a}$$

. On $\left[\dfrac{2k\pi - \angle G(j\omega_1)}{\omega_1} + \dfrac{\pi}{\omega_1}, \dfrac{2k\pi - \angle G(j\omega_1) + 2\pi}{\omega_1}\right]$, where $\dot{x}_{U_1,\omega_1}(t) > 0$ and $\dot{v}_{U_1,\omega_1}(t) > 0$, one has:

$$v_{U_1,\omega_1}(t) = V_{U_1}^+(x_{U_1,\omega_1}(t)). \tag{11b}$$

We will now make use of these properties to determine successively: (i) the phase $\angle G(j\omega_1)$ so that the signal $x_{U_1,\omega_1}(t)$ becomes fully known and; (ii) the two functions $(V_{U_1}^+, V_{U_1}^-)$ so that one can use them to build up an estimator of the hysteresis input signal $x(t)$ whenever this spans $[-U_1, U_1]$.

3.1.1 Estimation of the phase $\angle G(j\omega_1)$

Since $(V_{U_1}^+, V_{U_1}^-)$ are strictly increasing (by Assumption HLA), it follows from (11a-b) that $v_{U_1,\omega_1}(t)$ is in phase with $x_{U_1,\omega_1}(t)$. Then, within any $2\pi/\omega_1$-length time-interval, these two signals have a unique couple of extrema (one maximum and one minimum) that they achieve simultaneously (see Fig. 2a). Letting t_k $(k \in \mathbf{N})$ denote the instants where those extrema are achieved, it readily follows from (10a) that $\omega_1 t_k + \angle G(j\omega_1) = k\pi$, $k \in \mathbf{N}$. Then, bearing in mind (4), one gets the relationship:

$$\angle G(j\omega_1) = \begin{cases} -\omega_1 t_k & if\ -\omega_1 t_k \in [0,\pi) \\ -\omega_1 t_k + \pi & otherwise \end{cases}, \text{ modulo } 2\pi, \quad k \in \mathbf{N} \tag{12}$$

This shows that, $\angle G(j\omega_1)$ can be computed from one of the instants where the (undisturbed) output $v_{U_1,\omega_1}(t)$ achieves an extremum. As $v_{U_1,\omega_1}(t)$ is not accessible to measurement, it is replaced by its estimated signal $\bar{y}_{U_1,\omega_1,N}(t)$, obtained by operating the $2\pi/\omega_1$-periodic averaging (5a-b) on $y_{U_1,\omega_1}(t)$. Then, (12) suggests the following phase estimator:

$$\angle \hat{G}_N(j\omega_1) = \begin{cases} -\omega_1 t_{U_1,\omega_1,N} & if\ -\omega_1 t_{U_1,\omega_1,N} \in [0,\pi) \\ -\omega_1 t_{U_1,\omega_1,N} + \pi & if\ -\omega_1 t_{U_1,\omega_1,N} \in [\pi,2\pi) \end{cases} \quad (\text{modulo } 2\pi) \tag{13}$$

where $t_{U_1,\omega_1,N} \in [0, 2\pi/\omega_1]$ denotes any instant where $\bar{y}_{U_1,\omega_1,N}(t)$ achieves a maximum. Then, (10a) suggests the following estimator of $x_{U_1,\omega_1}(t)$:

$$\hat{x}_{U_1,\omega_1,N}(t) = U_1 \cos\left(\omega_1 t + \angle \hat{G}_N(j\omega_1)\right) \tag{14}$$

Proposition 1. The estimators $\angle \hat{G}_N(j\omega_1)$ and $\hat{x}_{U_1,\omega_1,N}(t)$ defined by (13) and (14), respectively, are consistent in the sense that one has w.p.1:

$$\angle \hat{G}_N(j\omega_1) - \angle G(j\omega_1) \underset{N\to\infty}{\to} 0, \text{ modulo } 2\pi \tag{15a}$$

$$\hat{x}_{U_1,\omega_1,N}(t) - x_{U_1,\omega_1}(t) \underset{N\to\infty}{\to} 0 \tag{15b}$$

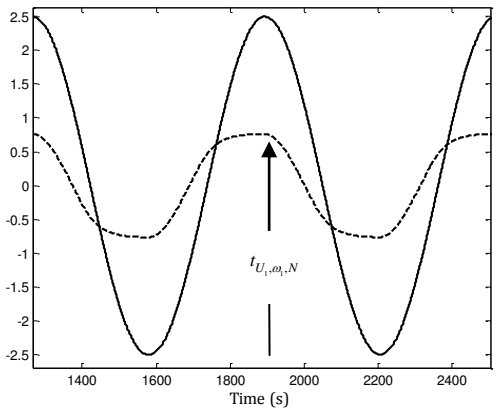

Fig. 2a. Steady-state response $v_{U_1,\omega_1}(t)$ (dashed) of a Bouc-

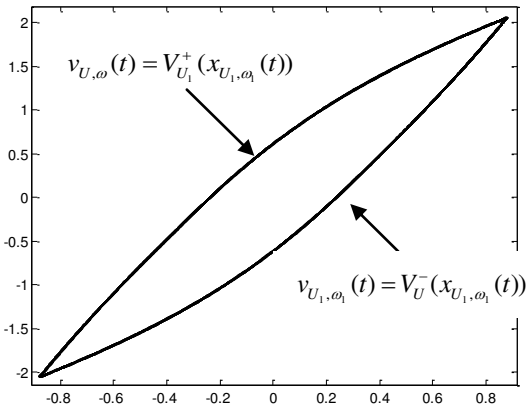

Fig. 2b. Hysteresis loop described by the working point $(x_{U_1,\omega_1}(t), v_{U_1,\omega_1}(t))$ associated to the experiment of

Wen hysteresis model (3a-b) to a sinusoidal signal $x_{U_1,\omega_1}(t)$ (solid). The hysteretic parameters are $\alpha=2, \beta=1, \gamma=0.4$, $\lambda_x=1$ and $\mu=1.5$ (see Section 5). Fig. 2a.

Proof of Proposition 1. By property (9), $\bar{y}_{U_1,\omega_1,N}(t)$ is constructively $2\pi/\omega_1$-periodic and $\bar{y}_{U_1,\omega_1,N}(t) \to v_{U_1,\omega_1}(t)$, w.p.1 as $N \to \infty$. Then, w.p.1 as $N \to \infty$, there exists a unique couple of times in $[0, 2\pi/\omega_1]$ where $\bar{y}_{U_1,\omega_1,N}(t)$ has extrema. Letting $t_{U_1,\omega_1,N}$ denote any one of these two times, it follows from (9) that that $t_{U_1,\omega_1,N}$ converges, w.p.1 as $N \to \infty$, to one of the t_k's where $v_{U_1,\omega_1}(t)$ achieves its extrema. Then, (15a) is obtained by comparing (12) and (13) . In turn, Property (15b) is got by comparing (14) and (10a) ■

3.1.2 Estimation of the hysteresis loop border functions $(V_{U_1}^+, V_{U_1}^-)$

By Assumption HLA, we know that the hysteresis working point $(x_{U_1,\omega_1}(t), v_{U_1,\omega_1}(t))$ generates a hysteresis loop, when t spans any interval of length $2\pi/\omega_1$ (see Fig. 2b). As pointed out by (11a-b), the two lateral bordering lines of this loop determine the border functions $(V_{U_1}^+, V_{U_1}^-)$. Then, substituting $(\hat{x}_{U_1,\omega_1,N}(t), \bar{y}_{U_1,\omega_1,N}(t))$ to $(x_{U_1,\omega_1}(t), v_{U_1,\omega_1}(t))$ in (11a-b), one gets an accurate estimate $(\hat{V}_{U_1,N}^+, \hat{V}_{U_1,N}^-)$ of the couple of functions $(V_{U_1}^+, V_{U_1}^-)$. Specifically, the estimated functions are defined as follows:

$$\begin{aligned} \hat{V}_{U_1,N}^+ : [-U_1, U_1] &\to \left] \min_t \bar{y}_{U_1,\omega_1,N}(t), \max_t \bar{y}_{U_1,\omega_1,N}(t) \right[\\ \hat{x}_{U_1,\omega_1,N}(t) &\to \bar{y}_{U_1,\omega_1,N}(t), \ \forall t \in \left(\frac{\pi - \angle \hat{G}_N(j\omega_1)}{\omega_1}, \frac{2\pi - \angle \hat{G}_N(j\omega_1)}{\omega_1} \right) \end{aligned} \tag{16a}$$

$$\begin{aligned} \hat{V}_{U_1,N}^- : [-U_1, U_1] &\to \left] \min_t \bar{y}_{U_1,\omega_1,N}(t), \max_t \bar{y}_{U_1,\omega_1,N}(t) \right[\\ \hat{x}_{U_1,\omega_1,N}(t) &\to \bar{y}_{U_1,\omega_1,N}(t), \ \forall t \in \left(\frac{-\angle \hat{G}_N(j\omega_1)}{\omega_1}, \frac{\pi - \angle \hat{G}_N(j\omega_1)}{\omega_1} \right) \end{aligned} \tag{16b}$$

where again we have used the fact that $\bar{y}_{U_1,\omega_1,N}(t)$ is constructively $2\pi/\omega_1$-periodic.

Proposition 2. The estimator defined by (16a-b) is consistent:

$$(\hat{V}_{U_1,N}^+, \hat{V}_{U_1,N}^-) \underset{N\to\infty}{\to} (V_{U_1}^+, V_{U_1}^-) \text{ (w.p.1)} \tag{17}$$

Proof. By Proposition 1, one knows that $\angle \hat{G}_N(j\omega_1)$ and $\hat{x}_{U_1,\omega_1,N}(t)$ are consistent estimators of $x_{U_1,\omega_1}(t)$ and $\angle G(j\omega_1)$. Also, by (9), $\bar{y}_{U_1,\omega_1,N}(t)$ is a consistent estimator of $v_{U_1,\omega_1}(t)$. Then, Proposition 2 follows directly from the comparison of (16a-b) and (11a-b) ■

3.2. Linear Subsystem Output Estimator

The estimation of the border functions $(V_{U_1}^+, V_{U_1}^-)$ constitutes a key achievement because these functions characterize all hysteresis loops generated by $F[\bullet]$ when this is excited by any input signal $x(t)$ that is loading-unloading spanning the interval $[-U_1, U_1]$. In the present context, the hysteresis input $x(t)$ is also the output of the Wiener system (1a). Since the function $(V_{U_1}^+, V_{U_1}^-)$ are strictly increasing, it becomes possible to accurately estimate the linear subsystem output $x(t)$ and, therefore, estimate the transfer function $G(s)$. Based on these observations, we let the Wiener system (1a-c) be excited by any input signal $u(t)$ such that the resulting (steady-state) signal $x(t)$ is T-periodic loading-unloading and spanning $[-U_1, U_1]$ (whatever the period T). It immediately follows from Assumption HLA that, in turn the resulting (steady-state) signal $v(t)$ is T-periodic loading-unloading and in phase with $x(t)$. More specifically, the two signals are related by expressions (2a-b) with $(V^+, V^-) = (V_{U_1}^+, V_{U_1}^-)$, the two functions identified in the previous subsection. Since these functions are invertible (because they are strictly increasing), equations (2a-b) entail the following relationship:

$$x(t) = \frac{1+\text{sgn}(\dot{v}(t))}{2}(V_{U_1}^+)^{-1}\big(v(t)\big) + \frac{1-\text{sgn}(\dot{v}(t))}{2}(V_{U_1}^-)^{-1}\big(v(t)\big) \tag{18}$$

This relation holds whenever $x(t)$ is loading-unloading spanning the interval $[-U_1, U_1]$. This suggests the following estimator for the signal $x(t)$:

$$\hat{x}_N(t) = \frac{1+\text{sgn}(\dot{\bar{y}}_N(t))}{2}(\hat{V}_{U_1,N}^+)^{-1}\big(\bar{y}_N(t)\big) + \frac{1-\text{sgn}(\dot{\bar{y}}_N(t))}{2}(\hat{V}_{U_1,N}^-)^{-1}\big(\bar{y}_N(t)\big) \tag{19}$$

where $\bar{y}_N(t)$ is obtained by applying (5a-b) to the output signal $y(t)$ of the Wiener system (1a-c) being excited by the above input $u(t)$.

Proposition 3. Consider the Wiener system (1a-c) subject to Assumptions HLA and (4). If the system input $u(t)$ is selected so that the resulting (steady-state) internal signal $x(t)$ is T-periodic loading-unloading and spanning the (known) interval $[-U_1, U_1]$ then, the estimator (19) is consistent, i.e.

$$\hat{x}_N(t) - x(t) \underset{N\to\infty}{\to} 0 \tag{20}$$

Proof. The proposition follows by comparing (19) and (18), using (9) and Proposition 2 ■

Remark 2. a) It is worth noting that the estimator (19) is applicable, whatever the shape of the input signal $u(t)$, provided the resulting internal signal $x(t)$ is T-periodic loading-unloading spanning the interval $[-U_1, U_1]$, whatever the value of the period T.

b) The estimator (19) involves the derivative of $\bar{y}_N$. The derivative exists w.p.1 because $\bar{y}_N$ is a consistent estimator of $v(t)$ which is differentiable. As $\bar{y}_N$ is bounded T-periodic, its derivative is

accurately approximated by the filtered signal $\frac{Ts}{1+Ts/M}\,y_N$ with $M >> 1$. The larger M the better the approximation.

3.3. Frequency Estimation of the Transfer Function $G(s)$

As $G(s)$ is of unknown structure, a frequency approach is proposed to estimate the frequency response $G(j\omega_i)$, for a set of frequencies ω_i $(i = 2\ldots n)$. The proposed approach entails the definition of a class Ω_a of admissible input signals.

Definition 2. An input signal $u(t)$ is said to belong to Ω_a if it meets the following requirements:

a) $u(t)$ is T-periodic spanning a symmetrical interval i.e. $\max_t u(t) = -\min_t u(t) \overset{def}{=} U_{\max}$.

b) The resulting linear subsystem output $x(t)$ is T-periodic loading-unloading and $\max_t x(t) = -\min_t x(t) \overset{def}{=} X_{\max}$. Furthermore, $X_{\max}$ is a strictly increasing continuous function of $U_{\max}$.

Remark 3. From Definition 2 it follows that the set Ω_a depends on the system transfer $G(s)$. Consequently, one should get benefit of any available prior knowledge on the system to determine elements the set Ω_a. This is illustrated in the next examples.

Example 2. a) When the transfer function $G(s)$ has finite-order and all its poles are with negative real parts, the set Ω_a includes (but is not limited to) all sinusoidal signals.

b) Let $G(s)$ be finite-order, strictly proper, with all poles and zeros being real negative scalars. Transfer functions satisfying these properties are asymptotically stable, minimum phase and non-oscillating. Then, the set Ω_a includes (in addition to those of Part a) all C^0 T-periodic signals such that: (i) there exists a scalar $0 < \kappa < 1$ so that u is C^1 strictly increasing on the open interval $(0, \kappa T)$ and C^1 strictly decreasing on the open interval $(\kappa T, T)$; (ii) the period T is sufficiently large (compared to the system rise-time). Among usual signals meeting these requirement, we can cite square waves with large periods compared to the system risetime.

In the rest of this section, it is assumed that the input signal $u \in \Omega_a$. Then, with the notation of Definition 2, the steady-state internal signal $x(t)$ is loading-unloading spanning a symmetrical interval $[-X_{\max}, X_{\max}]$ and $X_{\max}$ is a continuous strictly increasing function of $U_{\max}$. The key idea is to select the input amplitude $U_{\max}$ so that $[-X_{\max}, X_{\max}]$ coincides with $[-U_1, U_1]$ (the known interval introduced in subsection 3.1). Doing so, one can then make use of the estimator (19) to get an estimate of the inaccessible signal $x(t)$. By Assumption HLA, one can check that $x(t)$ spans $[-U_1, U_1]$ by

verifying whether the undisturbed output $v(t) = F[x](t)$ spans $[V^+(-U_1), V^+(U_1)]$. Based on these observations, we let the input amplitude $U_{\max}$ be selected so that the following statement holds:

$$\bar{y}_N(t) \text{ exactly spans the interval } [\hat{V}^+_{U_1,N}(-U_1), \hat{V}^+_{U_1,N}(U_1)] \tag{21}$$

where $\bar{y}_N(t)$ is the constructively T-periodic signal obtained by operating (5a-b) on the system output $y(t)$. Practically, the search for the value of $U_{\max}$ that meets the above requirement can be performed using the dichotomy rule of Table I, where the expression "$\bar{y}_N(t)$ spans a wider interval" means "wider than $[\hat{V}^+_{U_1,N}(-U_1), \hat{V}^+_{U_1,N}(U_1)]$. Analogous sense is given for "spans a narrower interval".

Table I. Selection of input amplitude $U_{\max}$

Let (U^0, U^1) denotes a pair of auxiliary real variables. Set $U_{\max} = U^0 = U_1$ where U_1 is as in (10a). Apply an input signal $u \in \Omega_a$ with amplitude $U_{\max}$ and compute $\bar{y}_N(t)$ by operating (5a-b) on $y(t)$. Execute the following dichotomy procedure to tune the value of $U_{\max}$:

1. If $\bar{y}_N(t)$ exactly spans $[\hat{V}^+_{U_1,N}(-U_1), \hat{V}^+_{U_1,N}(U_1)]$, keep on the value of $U_{\max}$ and quit the search procedure.
2. If $\bar{y}_N(t)$ spans a wider interval, let $U_{\max} = U_{\max}/2$, and go to Step 4.
3. If $\bar{y}_N(t)$ spans a narrower interval, let $U_{\max} = 2U_{\max}$ and go to Step 4.
4. If $\bar{y}_N(t)$ exactly spans $[\hat{V}^+_{U_1,N}(-U_1), \hat{V}^+_{U_1,N}(U_1)]$, keep on the value of $U_{\max}$ and quit the search procedure.
5. If $\bar{y}_N(t)$ spans a wider interval and $U_{\max} < U^0$, let $U^0 = U_{\max}$ and $U_{\max} = U_{\max}/2$, and go back to Step 4.
6. If $\bar{y}_N(t)$ spans a wider interval and $U_{\max} > U^0$, let $U^1 = U_{\max}$, $U_{\max} = (U_{\max} + U^0)/2$, $U^0 = U^1$ and go to Step 4.
7. If $\bar{y}_N(t)$ spans a narrower interval and $U_{\max} < U^0$, let $U^1 = U_{\max}$, $U_{\max} = (U_{\max} + U^0)/2$, $U^0 = U^1$ and go to Step 4.
8. If $\bar{y}_N(t)$ spans narrower interval and $U_{\max} > U^0$, let $U^0 = U_{\max}$ and $U_{\max} = 2U_{\max}$, and go to Step 4.

Once the input amplitude $U_{\max}$ is selected, one gets an accurate estimate $\hat{x}_N(t)$ of the internal signal $x(t)$, using (19) which (by Proposition 3) is consistent. As $x(t)$ is T-periodic (because $u \in \Omega_a$), it follows that $\hat{x}_N(t)$ admits a Fourier series expansion of the form:

$$\hat{x}_N(t) = \sum_{k=0}^{\infty} \hat{X}_{k,N} \cos\left(k\omega t + \hat{\phi}_{k,N}\right) + \delta_N(t), \text{ with } \omega = \frac{2\pi}{T} \tag{22}$$

where $\delta_N(t) \to 0$, w.p.1 as $N \to \infty$. Also, the T-periodic input $u(t)$ has a Fourier series of the form:

$$u(t) = \sum_{k=0}^{\infty} U_k \cos\left(k\omega t + \varsigma_k\right) \tag{23}$$

Then, the following frequency response estimator is considered:

$$\hat{G}_N(jk\omega) \overset{def}{=} \left|\hat{G}_N(jk\omega)\right| \exp\left(j\angle \hat{G}_N(jk\omega)\right) \tag{24}$$

with $\omega = \frac{2\pi}{T}$ and where:

$$\left|\hat{G}_N(jk\omega)\right| = \frac{\hat{X}_{k,N}}{U_k}, \quad \angle \hat{G}_N(jk\omega) = \hat{\phi}_{k,N} - \varsigma_k, \quad k \in \mathbf{N} \tag{25}$$

Proposition 4. 1) The statement (21) defines a unique value of $U_{\max}$ and the iterative search procedure of Table I converges to that value, w.p.1 as the number of iterations and N tends to infinity.

2) The frequency response estimator, defined by (24)-(25), is consistent:

$$\hat{G}_N(jk\omega) \underset{N\to\infty}{\to} G(jk\omega), \quad \text{w.p.1}, \quad k \in \mathbf{N} \tag{26}$$

See proof in Appendix B.

Remark 4. a) In addition to the estimates $\hat{G}_N(jk\omega)$ ($k \in \mathbf{N}$) that one obtains using a given T-periodic input $u \in \Omega_a$, other estimates can be obtained following similar steps, using another admissible input with different period.

b) As noticed in Example 2, in case where no prior knowledge on $G(s)$ is available, one can only use sinusoidal inputs $u(t) = U\cos(\omega_i t)$, $i = 2\ldots n$. As a matter of fact, applying the above method with $u(t) = U\cos(\omega_i t)$ only yields the frequency response estimate $\hat{G}_N(j\omega_i)$. Additional estimates are obtained by applying the identification method repeatedly with the different frequencies. Inversely, in the case where $G(s)$ meets the conditions of Example 2 (part b), one periodic input signal is sufficient to determine several frequency response estimates using (24)-(25).

c) Based on the above observations, it turns out that the identification of $G(s)$ only involves periodic input signals. Furthermore, the number of needed input signals depends on the properties of $G(s)$ and the available prior knowledge on it. The minimum number of input signals equals two: one sine input to construct the $x(t)$-estimator (19) and one periodic (not sine) signal to estimate the frequency response by (24)-(25). This is the case in the conditions of Example 2 (part b).

At this point, a set of frequency response values is available. Let it be denoted $\hat{G}_N(j\omega_i)$ $(1 = 1\ldots n)$, where ω_1 is as in (4). Now, suppose that the transfer function $G(s)$ is of known structure $G(s) = G(s, \theta_L)$ where θ_L is a vector including all unknown parameters. The aim is to estimate θ_L using the available frequency data $\hat{G}_N(j\omega_i)$. This problem has extensively been studied in past years and a number of solutions have been proposed, e.g. (Pintelon *et al.*, 1994; Schoukens *et al.*, 1998; Ljung, 1999). An example of such solutions is presented in Appendix C providing an estimate $\hat{\theta}_{L,N} \to \theta_L$, w.p.1 as $N \to \infty$.

The transfer function identification method thus constructed is recapitulated in Table II, where the following power norm is used:

$$\|z(t)\| \overset{def}{=} \left(\frac{1}{T}\int_0^T z(t)^2\, dt \right)^{1/2} \quad (z(t) \text{ any } T\text{-periodic signal}) \tag{27}$$

Table II. Summary of Transfer Function Identification Method

Step 1. **Hysteresis Loop Identification**

Data collection

1.1 Select a sine input $u(t)=U_1\cos(\omega_1 t)$, with $U_1>0, \omega_1\neq 0$, and choose a threshold $0<\varepsilon<<1$. The amplitude U_1 must be selected not too small so that a usable output is obtained despite noise. Apply the input signal $u(t)$ to the Wiener system (1a-c) and collect the steady-state output $y_{U_1,\omega_1}(t)$ over a sufficiently large interval, say $0\le t\le 2N\pi/\omega_1$ (with N large enough).

1.2. Generate the two periodic signals $\bar{y}_{U_1,\omega_1,N-1}(t)$ and $\bar{y}_{U_1,\omega_1,N}(t)$, by applying (5a-b) to $y_{U_1,\omega_1}(t)$, and compute the following relative errors, using the power norm defined by (27) letting there $T=2\pi/\omega_1$:

$$e_1(N)\overset{def}{=}\left\|\bar{y}_{U_1,\omega_1,N}(t)-\bar{y}_{U_1,\omega_1,N-1}(t)\right\|/\left\|\bar{y}_{U_1,\omega_1,N}(t)\right\| \quad \text{and} \quad e_2(N)=\left\|\bar{y}_{U_1,\omega_1,N}(t)-\overset{def}{\bar{y}}_{U_1,\omega_1,N}(t-2\pi/\omega_1)\right\|/\left\|\bar{y}_{U_1,\omega_1,N}(t)\right\|.$$

If $e_1(N)<\varepsilon$ and $e_2(N)<\varepsilon$ then, go to Step 1.3. Otherwise, increase N and repeat Step 1.2.

Hysteresis loop estimation

1.3. To estimate $\hat{x}_{U_1,\omega_1,N}(t)$, let $0\le t_{U_1,\omega_1,N}\le 2\pi/\omega_1$ be any time instant where $\bar{y}_{U_1,\omega_1,N}(t)$ achieves an extremum. Using (13) get the estimate $\angle\hat{G}_N(j\omega_1)$ and by (14) get $\hat{x}_{U_1,\omega_1,N}(t)=U_1\cos\left(\omega_1 t+\angle\hat{G}_N(j\omega_1)\right)$.

1.4. Using $(\hat{x}_{U_1,\omega_1,N}(t),\bar{y}_{U_1,\omega_1,N}(t));(0\le t<2\pi/\omega_1)$, construct the hysteresis loop border functions $(\hat{V}^+_{U_1,N},\hat{V}^-_{U_1,N})$ by applying (16a-b). Then, construct the estimator (19) of the linear subsystem output.

Step 2. Transfer Function Estimation.

2.1. With the notations of Definition 2, select an admissible input signal $u\in\Omega_a$, with period $T>0$ and amplitude $U_{\max}$. Tune the latter using the search procedure of Table I.

2.2. Using (19), get $\hat{x}_N(t)$ and, using (22)-(25), get the estimates $\hat{G}_N(jk\omega)$ $(k=1,2,3\ldots)$.

2.3. If $G(s)$ is of known structure, get the parameter vector estimate $\hat{\theta}_{L,N}$ using e.g. the method in Appendix C.

Remark 5. a) In Step 1.2 of Table II, the tests on $e_1(N)$ and $e_2(N)$ are resorted for searching a suitable averaging horizon N to be used in (5a-b). By (9), the search in Step 1.2, is guaranteed to converge in finite time. Similarly, Part 1 of Proposition 4 guarantees that the search of input amplitude $U_{\max}$ in Step 2.1 does converges as the number of iterations goes to ∞. To ensure a convergence after a finite number of iterations, it suffices to replace in Table I $[\hat{V}^+_{U_1,N}(-U_1),\hat{V}^+_{U_1,N}(U_1)]$ by $[\hat{V}^+_{U_1,N}(-U_1)-\upsilon,\hat{V}^+_{U_1,N}(U_1)+\upsilon]$, for some $0<\upsilon<<1$.

b) Suppose the transfer function $G(s,\theta_L)$ is of known structure and the available prior knowledge on it is such that one can select an admissible input $u\in\Omega_a$ not limited to sine type. This is e.g. the case in Part b of Example 2. Then, the parameter identification of $G(s,\theta_L)$ can be directly performed without passing by the estimation of frequency response values $\hat{G}_N(jk\omega)$. For instance, assume that $x=G(s,\theta_L)u$ is equivalent to $A(s,\theta_L)x(t)=B(s,\theta_L)u(t)$, where $A(s,\theta_L)$ and $B(s,\theta_L)$ are polynomials of known structure and θ_L is the vector including their coefficients. Then, θ_L enters linearly in the previous autoregressive representation making the standard LS estimator usable. Obviously, the inaccessible signal $x(t)$ should be replaced by its consistent estimate $\hat{x}_N(t)$, leading to a consistent parameter estimator of $\hat{\theta}_{L,N}$. In this regard, note that $u(t)$ is persistently exciting because it is T-periodic (By Definition 2) and, as emphasized by (23), its power spectrum includes an infinite number of frequencies.

4. HYSTERESIS PARAMETER IDENTIFICATION

The result of Section 3 is a quite useful as it shows that the linear subsystem with transfer function $G(s)$ can be identified first. As long as the identification of $G(s)$ is concerned, no prior knowledge is required on the hysteretic operator $F[\bullet]$ except for Assumption HLA. In this section, it is shown that the inverse is (almost) true. Specifically, the nonlinear hysteretic operator can be identified without using the available estimate of $G(s)$, except for (the estimate of) its static gain $G(0)$. This is illustrated by considering the Bouc-Wen hysteresis model (3a-b). Of course, one could alternately use more standard methods making full use of (the estimate of) $G(s)$. Such identification methods are available e.g. for Bouc-Wen model (Ikhouane and Gomis-Bellmunt, 2008), Prandtl-Ishlinkskii model (Kuhnen, 2003), and Preisach model (Tan X. and J.S. Baras, 2005).

4.1 Bouc-Wen Model Re-Parameterization

Without loss of generality the Bouc-Wen model (3a-b) entails an equivalent representation of the form:

$$\dot{w}(t) = \alpha\dot{x}(t) - \beta\left|\dot{x}(t)\right|\left|w(t)\right|^{\mu-1}w(t) - \gamma\dot{x}(t)\left|w(t)\right|^{\mu} \tag{28}$$

$$v(t) = \lambda_x x(t) + w(t) \tag{29}$$

This representation features a smaller number of unknown parameters as the coefficient λ_w in (3b) is set to 1 in (29). Of course, the parameters (α, β, γ) and the internal signal $w(t)$ in (28)-(29) are not identical to the corresponding parameters and internal signal in (3a-b). The same symbols are used in (28)-(29) just to avoid introducing extra notation. Also, to alleviate the presentation, the derivation of (28)-(29) is placed in Appendix A. The following proposition completes the model (28)-(29).

Proposition 5. The Bouc-Wen model (28)-(29) satisfies Assumption HLA. Furthermore, the hysteresis internal state $w(t)$ has similar steady-state properties as $v(t)$ in HLA. In particular, $w(t)$ is T-periodic loading-unloading and the set $\{(x(t), w(t)); t \geq 0\}$ is an oriented closed locus, referred to as (x, w)-hysteresis loop, bordered by strictly increasing border functions (W^+, W^-).

See proof in (Ikhouane and Rodellar, 2007, ch. 2). Additional properties are found in Appendix A where Fig. A1 emphasizes the system series-parallel structure of the Wiener system (1a-c) and (28)-(29), making the parameters $(\alpha, \beta, \gamma, \mu, \lambda_x)$ enter nonlinearly because $(x(t), v(t), w(t))$ are inaccessible.

4.2 Estimation of the parameter λ_x

We will again make use of the (steady-state) system output $y_{U_1,\omega_1}(t)$ to the input $u_1(t) = U_1\cos(\omega_1 t)$ (see Subsection 3.1). These signals are related by equations (10a-c) where (10b) must now be replaced by (28)-(29). For convenience, the expressions of interest are rewritten:

$$x_{U_1,\omega_1}(t) = U_1\cos\left(\omega_1 t + \angle G(j\omega_1)\right) \tag{30a}$$

$$\dot{x}_{U_1,\omega_1}(t) = -U_1\omega_1 \sin\left(\omega_1 t + \angle G(j\omega_1)\right) \tag{30b}$$

$$\dot{w}_{U_1,\omega_1} = \alpha \dot{x}_{U_1,\omega_1} - \beta\left|\dot{x}_{U_1,\omega_1}\right|\left|w_{U_1,\omega_1}\right|^{\mu-1} w_{U_1,\omega_1} - \gamma \dot{x}_{U_1,\omega_1}\left|w_{U_1,\omega_1}\right|^{\mu} \tag{30c}$$

$$v_{U_1,\omega_1}(t) = \lambda_x x_{U_1,\omega_1}(t) + w_{U_1,\omega_1}(t), \tag{30d}$$

$$y_{U_1,\omega_1}(t) = v_{U_1,\omega_1}(t) + \xi(t) \tag{30e}$$

Presently, an additional experiment is performed considering the shifted input $u_1^{sh}(t) = U_1\cos(\omega_1 t) + U_{sh}$, with $U_{sh} > 0$ is freely chosen by the user, where the script '*sh*' refers to 'shifted' signals and scalars. Letting $(x^{sh}_{U_1,\omega_1}, w^{sh}_{U_1,\omega_1}, v^{sh}_{U_1,\omega_1}, y^{sh}_{U_1,\omega_1})$ denote the associated responses, the following expressions (analogous to (30a), (30d) and (30e)) are readily obtained from (1a), (1c) and (29):

$$x^{sh}_{U_1,\omega_1}(t) = U_1\cos\left(\omega_1 t + \angle G(j\omega_1)\right) + \left|G(0)\right|U_{sh} = x_{U_1,\omega_1}(t) + \left|G(0)\right|U_{sh} \tag{31a}$$

$$v^{sh}_{U_1,\omega_1}(t) = \lambda_x x^{sh}_{U_1,\omega_1}(t) + w^{sh}_{U_1,\omega_1}(t) \tag{31b}$$

$$y^{sh}_{U_1,\omega_1}(t) = v^{sh}_{U_1,\omega_1}(t) + \xi^{sh}(t) \tag{31c}$$

where $\xi^{sh}(t)$ denotes the realization of the output noise during the new experiment. Subtracting (30d) from (31b) and (30e) from (31c), one gets:

$$v^{sh}_{U_1,\omega_1}(t) - v_{U_1,\omega_1}(t) = \lambda_x\left|G(0)\right|U_{sh} \tag{32a}$$

$$y^{sh}_{U_1,\omega_1}(t) - y^{sh}_{U_1,\omega_1}(t) = \lambda_x\left|G(0)\right|U_{sh} + (\xi^{sh}(t) - \xi(t)) \tag{32b}$$

Operating the periodic averaging (5a-b) on both sides of (32b), one gets:

$$\overline{y}^{sh}_{U_1,\omega_1,N}(t) - \overline{y}_{U_1,\omega_1,N}(t) = \lambda_x\left|G(0)\right|U_{sh} + (\overline{\xi}^{sh}_N(t) - \overline{\xi}_N(t)) \tag{32c}$$

Averaging both sides of (32c) over the interval $[0, T_1]$, with $T_1 = 2\pi/\omega_1$, gives:

$$\lambda_x = \frac{1}{\left|G(0)\right|U_{sh}}\frac{1}{T_1}\int_0^{T_1}(\overline{y}^{sh}_{U_1,\omega_1,N}(t) - \overline{y}_{U_1,\omega_1,N}(t))dt + \frac{1}{\left|G(0)\right|U_{sh}}\frac{1}{T_1}\int_0^{T_1}(\overline{\xi}^{sh}_N(t) - \overline{\xi}_N(t))dt \tag{33a}$$

This suggests the following estimator of λ_x:

$$\hat{\lambda}_{x,N} = \frac{1}{\left|\hat{G}_N(0)\right|U_{sh}}\frac{1}{T_1}\int_0^{T_1}(\overline{y}^{sh}_{U_1,\omega_1,N}(t) - \overline{y}_{U_1,\omega_1,N}(t))dt; \tag{33b}$$

where $\hat{G}_N(0)$ is readily obtained letting $s = 0$ in the transfer function estimate $G(s, \hat{\theta}_{L,N})$ obtained in Section 3.3. Comparing (33a) and (33b), it is readily seen that:

$$\hat{\lambda}_{x,N} \underset{N\to\infty}{\to} \lambda_x \quad \text{(w.p. 1)} \tag{34}$$

where we have used the zero-mean ergodicity of output noise $\xi(t)$ and the fact that $\hat{G}_N(0)$ is a consistent estimator of $G(0)$ (because $\hat{\theta}_{L,N}$ is a consistent estimator of θ_L (see Proposition C1 in Appendix C).

Remark 6. Equation (32b) shows that the parameter λ_x is identifiable provided that $G(0) \neq 0$. Practically, this assumption is not very restrictive because real-life systems with zero static-gain are rather the exception than the rule.

4.2 Estimation of the parameters $(\alpha, \beta, \gamma, \mu)$

The estimation of the parameters $(\alpha, \beta, \gamma, \mu)$ will now be performed on the basis of equation (30c). Accordingly, no additional data acquisition will be required (those already collected in Subsection 3.1, using the input signal $u(t) = U_1 \cos(\omega_1 t)$, will prove to be sufficient). Now, to make use of (30c) one needs to replace all inaccessible signals involved there by their estimates. Equation (30d), suggests the following estimator of $w_{U_1,\omega_1}(t)$:

$$\hat{w}_{U_1,\omega_1,N}(t) = \bar{y}_{U_1,\omega_1,N}(t) - \hat{\lambda}_{x,N}\hat{x}_{U_1,\omega_1,N}(t) \tag{35}$$

with $\hat{x}_{U_1,\omega_1,N}(t) = U_1 \cos\left(\omega_1 t + \angle\hat{G}_N(j\omega_1)\right)$ where $\bar{y}_{U_1,\omega_1,N}(t)$ is obtained by (5a-b). Clearly, $\hat{w}_{U_1,\omega_1,N}(t)$ is a consistent estimator of $w_{U_1,\omega_1}(t)$ because, $\bar{y}_{U_1,\omega_1,N}(t)$, $\hat{\lambda}_{x,N}$ and $\angle\hat{G}_N(j\omega_1)$ are known (by (9), (34), and (15a)) to be consistent estimators of $v_{U_1,\omega_1}(t)$, λ_x, and $\angle G(j\omega_1)$, respectively. The point is that equation (30c) also involves the derivative of $w_{U_1,\omega_1}(t)$. This derivative cannot be obtained from (35) because this involves $\bar{y}_{U_1,\omega_1,N}(t)$ which, by (5a-b) and (30e), depends on the noise $\xi(t)$ which is not necessarily differentiable. To get around this difficulty, equation (30c) is transformed by operating the filter $D(s) = 1/(1+T_D s)$ on both sides of it, with $0 < T_D << 2\pi/\omega_1$. Doing so, one gets:

$$\begin{aligned} w^D_{U_1,\omega_1} &= \alpha x^D_{U_1,\omega_1} - \beta D(s)\left(\left|\dot{x}_{U_1,\omega_1}\right| w_{U_1,\omega_1}\right|^{\mu-1} w_{U_1,\omega_1}\right) - \gamma D(s)\left(\dot{x}_{U_1,\omega_1}\left|w_{U_1,\omega_1}\right|^{\mu}\right) \\ &\overset{def}{=} \psi^T(\mu,t)\theta_H \end{aligned} \tag{36a}$$

with

$$w^D_{U_1,\omega_1} = sD(s)[w_{U_1,\omega_1}], \quad x^D_{U_1,\omega_1} = sD(s)[x_{U_1,\omega_1}] \tag{36b}$$

where the parameter vector $\theta_H \in \mathbf{R}^3$ and the regressor $\psi(\mu,t) \in \mathbf{R}^3$ are defined by:

$$\theta_H = \begin{bmatrix} \alpha & \beta & \gamma \end{bmatrix}^T \tag{36c}$$

$$\psi(\mu,.) = \begin{bmatrix} x^D_{U_1,\omega_1} & -D(s)[\left|\dot{x}_{U_1,\omega_1}\right| w_{U_1,\omega_1}\right|^{\mu-1} w_{U_1,\omega_1}] & -D(s)[\dot{x}_{U_1,\omega_1}\left|w_{U_1,\omega_1}\right|^{\mu}] \end{bmatrix}^T \tag{36d}$$

To see the benefit of equation (36a) (over (30c)), let the signals $x_{U_1,\omega_1}(t)$, $\dot{x}_{U_1,\omega_1}(t)$, $w_{U_1,\omega_1}(t) = v_{U_1,\omega_1}(t) - \lambda_x x_{U_1,\omega_1}(t)$ be temporarily assumed to be known (i.e. accessible to measurements). Then, it follows from (36b) that all quantities in (36a) can be computed because the filters $D(s) = 1/(1+T_D s)$ and $sD(s) = s/(1+T_D s)$ are realizable (as both are known and proper).

On the other hand, it is readily seen that equation (36a) involves two unknown quantities, the vector θ_H and the scalar $\mu > 1$. Furthermore, the former has the properties $\alpha \geq 0$, $\beta > 0, \gamma > 0$, $\beta + \gamma > 0$ and $\beta - \gamma \geq 0$ (see Example 1). It follows that:

$$\theta_H \in \boldsymbol{C} \text{ with } \boldsymbol{C} = \left\{ [\theta_1 \ \theta_2 \ \theta_3]^T \in \mathbf{R}^3 \middle| \ \theta_1 \geq 0, \theta_2 - \theta_3 \geq 0, \theta_2 + \theta_3 \geq 0 \right\} \tag{37}$$

Clearly, $\boldsymbol{C}$ is a convex set. The above observations motivate the introduction of the following optimization problem:

$$\min_{\eta > 1, \theta \in \boldsymbol{C}} J(\eta, \theta) \tag{38a}$$

with

$$J(\eta, \theta) = \int_{2k\pi/\omega_1}^{2(k+1)\pi/\omega_1} \left(w^D_{U_1,\omega_1}(t) - \theta^T \psi(\eta, t) \right)^2 dt \tag{38b}$$

where $k \in \mathbf{N}$ is any sufficiently large integer (recall that $w_{U_1,\omega_1}(t)$ is steady-state $2\pi/\omega_1$-periodic). It readily follows from (36a) and (38b) that $J(\mu, \theta_H) = 0$, i.e. $J(\eta, \theta)$ does achieve its global minimum at $(\eta, \theta) = (\mu, \theta_H)$. The question is whether this global minimum is solely achieved with (μ, θ_H). The uniqueness of this global minimum is formally established in Proposition 6 (see hereafter). So, it will remain to design a search method for determining the unique solution (μ, θ_H) of this optimisation problem. The main difficulty is that the function $J(\eta, \theta)$ is quadratic in θ but not in η (this is clearly seen in (36d)). Then, the optimization problem (38a-b) will be coped with using the separable least-squares technique which, in fact, is a form of relaxation. Accordingly, one temporarily assumes that η is known in (38b) so that (38a) becomes a least-squares problem, whose solution is,

$$\Pi_{LS}(\eta) = \left(\int_{2k\pi/\omega_1}^{2(k+1)\pi/\omega_1} \psi(\eta, t) \psi^T(\eta, t) dt \right)^{-1} \int_{2k\pi/\omega_1}^{2(k+1)\pi/\omega_1} w^D_{U_1,\omega_1}(t) \psi(\eta, t) dt \tag{39}$$

where $k \in \mathbf{N}$ is as in (38b). At this point, it is worth noticing that, if μ is substituted to η in (39) then one gets θ_H, using (36b). Specifically, one has:

$$\theta_H = \Pi_{LS}(\mu) = \left(\int_{2k\pi/\omega_1}^{2(k+1)\pi/\omega_1} \psi(\mu, t) \psi^T(\mu, t) dt \right)^{-1} \int_{2k\pi/\omega_1}^{2(k+1)\pi/\omega_1} w^D_{U_1,\omega_1}(t) \psi(\mu, t) dt \tag{40}$$

Now, let us go back to (38b) and replace there θ by $\Pi_{LS}(\eta)$ using (39). Doing so, one gets a one-dimensional optimisation problem, that only involves the variable η:

$$\min_{\eta > 1} I(\eta) \tag{41a}$$

$$I(\eta) \overset{def}{=} J(\eta, \Pi_{LS}(\eta)) = \int_{2k\pi/\omega}^{2(k+1)\pi/\omega} \left(w^D_{U_1,\omega_1}(t) - \Pi_{LS}(\eta)^T \psi(\eta, t) \right)^2 dt \tag{41b}$$

Note that, for this problem to be well posed, the function $\Pi_{LS}(\eta)$ must be well defined which presently means that the matrix (that needs to be inversed) on the right side of (39) is actually invertible, whatever $\eta > 1$. The invertibility of that matrix is formally proved in the proof of

Proposition 6 (Part 2). This makes it possible to apply the separable least-squares technique which operates this way: first, minimize $I(\eta)$ and denote $\hat{\mu}$ the value where the minimum is reached; then substituting $\hat{\mu}$ to μ in (40) one gets an estimate $\hat{\theta}_H = \Pi_{LS}(\hat{\mu})$ of θ_H.

Proposition 6. 1) The optimization problem (38a-b), involving the cost function $J(\eta,\theta)$ has a unique solution, namely: $\arg\min_{\eta>1,\theta\in C} J(\eta,\theta) = (\mu,\theta_H)$.

2) In turn, the optimization problem (41a-b), involving the cost function $I(\eta)$, has a unique solution, namely: $\arg\min_{\eta>1} I(\eta) = \mu$.

See proof in Appendix D. The above result is quite important. But, it still is not quite practical because the function $I(\eta)$ involves unavailable signals, i.e. $w^D_{U_1,\omega_1}(t)$ and $\psi(\eta,t)$ (see (41a-b)). Nevertheless, a practical cost function is readily obtained by replacing in $I(\eta)$ the unavailable signals by their estimates. Doing so, one gets the following cost function:

$$I_N(\eta) = \int_0^{2\pi/\omega} \left(\hat{w}^D_{U_1,\omega_1,N}(t) - \Pi_{LS,N}(\eta)^T \psi_N(\eta,t)\right)^2 dt \tag{42}$$

with:

$$\hat{w}^D_{U_1,\omega_1,N} = sD(s)[\hat{w}_{U_1,\omega_1,N}];\ \ \hat{w}_{U_1,\omega_1,N}(t) = \bar{y}_{U_1,\omega_1,N}(t) - \hat{\lambda}_{x,N}\hat{x}_{U_1,\omega_1,N}(t) \tag{43}$$

$$\Pi_{LS,N}(\eta) = \left(\int_0^{2\pi/\omega_1} \psi_N(\eta,t)\psi_N^T(\eta,t)dt\right)^{-1} \int_0^{2\pi/\omega_1} \hat{w}^D_{U_1,\omega_1,N}(t)\psi_N(\eta,t)dt \tag{44}$$

$$\psi_N(\eta,.) = \left[\hat{x}^D_{U_1,\omega_1,N} \quad -D(s)[\left|\dot{\hat{x}}_{U_1,\omega_1,N}\right|\left|\hat{w}_{U_1,\omega_1,N}\right|^{\eta-1}\hat{w}_{U_1,\omega_1,N}] - D(s)[\dot{\hat{x}}_{U_1,\omega_1,N}\left|\hat{w}_{U_1,\omega_1,N}\right|^{\eta}]\right]^T \tag{45a}$$

$$\hat{x}^D_{U_1,\omega_1,N} = sD(s)[\hat{x}_{U_1,\omega_1,N}],\ \ \hat{x}_{U_1,\omega_1,N}(t) = U_1\cos\left(\omega_1 t + \angle\hat{G}_N(j\omega_1)\right) \tag{45b}$$

where we have used the fact that all involved signals are $2\pi/\omega_1$-periodic (by (5a-b)), letting the integrals in (44) be computed on $[0,2\pi/\omega_1]$. With the above notations, the (μ,θ_H)-estimator is expressed as follows:

$$\hat{\mu}_N = \arg\min_{\eta>1} I_N(\eta) \tag{46a}$$

$$\hat{\theta}_{H,N} = P_{\boldsymbol{C}}(\Pi_{LS,N}(\hat{\mu}_N)) \tag{46b}$$

where the operator $P_{\boldsymbol{C}}(.)$ denotes the orthogonal projection on the set $\boldsymbol{C}$. This projection improves the quality of the estimates $\hat{\theta}_{H,N}$ because $\theta_H \in \boldsymbol{C}$ and $\boldsymbol{C}$ is convex, ensuring $\left\|\hat{\theta}_{H,N} - \theta_H\right\| \le \left\|\Pi_{LS,N}(\hat{\mu}_N) - \theta_H\right\|$.

Proposition 7. The estimator (46a-b) is consistent i.e. $(\hat{\mu}_N, \hat{\theta}_{H,N})$ converges to (μ,θ_H), w.p.1, as $N \to \infty$.

Proof. The key fact is that the estimators $\bar{y}_{U_1,\omega_1,N}$ and $\angle\hat{G}_N(j\omega_1)$, respectively defined by (5a-b) and (13), are consistent in the sense that the former converges (by (9)) to $v_{U_1,\omega_1}(t)$ and the latter converges (by (15a)) to $\angle G(j\omega_1)$, w.p.1 as $N\to\infty$. Then, comparing the quantities in (36a-d) and (39) with the corresponding quantities in (42)-(45b), it follows that $\psi_N(\eta,t)$ and $\Pi_{LS,N}(\eta)$ converge (w.p.1 as $N\to\infty$) to $\psi(\eta,t)$ and $\Pi_{LS}(\eta)$, respectively. Then, comparing (41b) and (42), one sees that $I_N(\eta)$ converges to $I(\eta)$ (w.p.1 as $N\to\infty$). Then, it follows using Proposition 6 that, $\hat{\mu}_N$ converges to μ and $\hat{\theta}_{H,N}$ to $\Pi_{LS}(\mu)=\theta_H$, w.p.1 as $N\to\infty$ ■

The hysteretic subsystem identification method thus designed is summarized in Table III.

Table III. Hysteretic subsystem identification method

Step 1. Data collection.

1.1 Again, consider the data collected in Table II (Step 1).

1.2 Collect also the system output $y^*_{U_1,\omega_1}(t)$ to the input signal $u_1^{sh}(t)=U_1\cos(\omega_1 t)+U_{sh}$, over $0\le t\le 2N\pi/\omega_1$, and compute the associated signal $\bar{y}^{sh}_{U_1,\omega_1,N}(t)$ using (5a-b).

Step 2. Estimation of the parameter λ_x. Compute the estimate $\hat{\lambda}_{x,N}$ using the estimator (33b)

Step 3. Estimation of the parameter vector $\theta_H=[\alpha\quad\beta\quad\gamma]^T$.

3.1. Compute $\dot{\hat{x}}_{U_1,\omega_1}(t)=-U_1\omega_1\sin\left(\omega_1 t+\angle\hat{G}_N(j\omega_1)\right)$ and the filtered signals $\hat{x}^D_{U_1,\omega_1,N}$, $\hat{w}^D_{U_1,\omega_1,N}$ using (43) and (45b).

3.2. Construct the vector function $\Pi_{LS,N}(\eta)$ using (44) and the scalar function $I_N(\eta)$ using (42).

3.3. Determine the global minimum of $I_N(\eta)$, e.g. by plotting $I_N(\eta)$ vs $\eta>1$.

3.4. Compute the parameter estimates $\hat{\theta}_{H,N}=\left[\hat{\alpha}_N\quad\hat{\beta}_N\quad\hat{\gamma}_N\right]^T$ using (46b).

5. SIMULATION

Let the system (1a-c) be characterized by $G(s)=0.1/(s+0.5)(s+0.2)$ and a hysteretic operator $F[.]$ described by (28)-(29) with the parameters $\alpha=2,\beta=1,\gamma=0.4,\lambda_x=1$ and $\mu=1.5$. The noise $\xi(t)$ is a normally distributed random signal, with zero mean and standard deviation $\sigma_\xi=0.1$.

5.1 Identification of the linear subsystem transfer function $G(s)$

Following Table II, the system transfer function $G(s)$ is identified in two main steps.

Hysteresis loop identification. According to Table II, the first step consists in identifying the hysteresis loop produced when the Wiener system is excited with a sine input $u(t)=U_1\cos(\omega_1 t)$. Presently, the choice $U_1=1$ and $\omega_1=0.02\,rd/s$ is made. The resulting steady-state output signal $y_{U_1,\omega_1}(t)$ is shown by Fig. 3a and its filtered version $\bar{y}_{U_1,\omega_1,N}(t)$, obtained by applying (5a-b) to $y_{U_1,\omega_1}(t)$ with $N=200$, is plotted in Fig. 3b. This shows that $\bar{y}_{U_1,\omega_1,N}(t)$ achieves an extremum at time $\bar{t}_{U_1,\omega_1,N}=7.5s$. Applying (13), one gets the phase estimate $\angle\hat{G}_N(j\omega_1)=-0.15\ (rad)$ and the estimated (linear subsystem output) signal $\hat{x}_{U_1,\omega_1,N}(t)=U_1\cos\left(\omega_1 t+\angle\hat{G}_N(j\omega_1)\right)$. Then, plotting the locus

$(\hat{x}_{U_1,\omega_1,N}(t), \bar{y}_{U_1,\omega_1,N}(t)); (0 \le t < 2\pi/\omega_1)$, one gets the hysteresis loop of Fig. 4. The borders of this hysteresis loop define two functions $v = \hat{V}^+_{U_1,N}(x)$ and $v = \hat{V}^-_{U_1,N}(x)$. One needs the corresponding inverse functions, $x = (\hat{V}^+_{U_1,N})^{-1}(v)$ and $x = (\hat{V}^-_{U_1,N})^{-1}(v)$. Presently, the inverse functions are captured through an orthogonal function series expansion, involving Legendre orthogonal polynomials, on $\left[\hat{V}^+_{U_1,N}(-U_1), \hat{V}^+_{U_1,N}(U_1)\right] = [-2.21, 2.21]$. The obtained inverse functions serve to construct the (linear subsystem) output estimator (19), used in the next subsection.

Identification of $G(s)$. First, no prior knowledge on $G(s)$ is supposed to be available. As pointed out in Example 2 (Part a) and Remark 4 (Part b), sinusoidal input signals $u(t) = U_i \cos(\omega_i t)$ $(i = 1 \ldots n)$ are resorted to get the estimates of a set of frequency response $G(j\omega_i)$. The frequencies are freely chosen, while the input amplitudes are selected using the search procedure of Table I. Then, the estimates $\hat{G}_N(j\omega_i)$ are obtained using (19) and (22)-(25). Let us illustrate the method (in Step 2 of Table II) for $(U_2, \omega_2) = (1.03, 0.05\ rd/s)$. The output $y_{U_2,\omega_2}(t)$ is collected, on $0 \le t \le 2N\pi/\omega_2$ (with $N = 200$), and its filtered version $\bar{y}_{U_2,\omega_2,N}(t)$ is obtained applying (5a-b). Both signals are depicted in Fig. 5a-b. Notice that $\bar{y}_{U_2,\omega_2,N}(t)$ exactly spans the interval $[\hat{V}^+_{U_1,N}(-U_1), \hat{V}^+_{U_1,N}(U_1)] = [-2.21, 2.21]$. In fact, the value $U_2 = 1.03$ has been selected (using Table I) so that full spanning of the above interval by $\bar{y}_{U_2,\omega_2,N}(t)$ is observed. Using (19), one gets the estimate $\hat{x}_{U_2,\omega_2,N}(t)$ of the internal signal $x_{U_2,\omega_2}(t)$. The true and estimated signals are plotted in Fig. 6. Then, the frequency response estimate $\hat{G}_N(j\omega_2)$ is obtained using (24)-(25) letting there $k = 1$ and $\omega = \omega_2$. This procedure is repeated with various couples (U_i, ω_i). A sample of the estimates $\hat{G}_N(j\omega_i)$ thus obtained is shown in Table IV. This shows that all estimates are quite close to their true values. Now, let us assume the structure of $G(s)$ to be known. Then, the corresponding parameter vector is $\theta_L = [0.7\ 0.1\ 0.1]^T$. Applying the estimation method of Appendix C, one gets the estimate $\hat{\theta}_{L,N} = [0.68\ 0.103\ 0.105]^T$.

Estimation of the hysteretic subsystem parameters

In the second stage of the identification method, the hysteresis parameters are estimated. Following Table III, the input signal $u(t) = U_1 \cos(\omega_1 t)$ and the corresponding system output $y_{U_1,\omega_1}(t)$ are used again. These are completed with new data including the (shifted-amplitude) input signal $u^{sh}(t) = U_1 \cos(\omega_1 t) + U_{sh}$ and the corresponding system output $y^{sh}_{U_1,\omega_1}(t)$. All signals are collected over the interval $0 \le t \le 2N\pi/\omega_1$ with $N = 200$. Using these data, an estimate of the parameter λ_x is readily obtained using (33b). Doing so, one gets $\hat{\lambda}_{x,N} = 0.97$ which is close to the true value $\lambda_x = 1$.

Then, the filtered signals $\hat{x}^D_{U_1,\omega_1,N}, \hat{w}^D_{U_1,\omega_1,N}$ are computed using (43) and (45b) with $D(s) = 1/(1+s)$. For the sake of illustration, both $w^D_{U_1,\omega_1}$ and $\hat{w}^D_{U_1,\omega_1,N}$ are plotted in Fig. 7 which confirms the satisfactory quality of the estimation. Then, the vector function $\Pi_{LS,N}(\eta)$ is constructed using (44) and the scalar function $I_N(\eta)$ using (42). The latter is plotted in Fig. 8 which confirms that $I_N(\eta)$ features a global minimum, achieved at $\hat{\mu}_N \approx 1.55$. Then, using (46b), one gets the hysteresis parameter estimate $\hat{\theta}_{H,N} = \left[\hat{\alpha}_N \quad \hat{\beta}_N \quad \hat{\gamma}_N\right]^T = \left[2.05 \quad 1.04 \quad 0.403\right]^T$ which is close to the true vector $\theta_H = \left[2 \quad 1 \quad 0.4\right]^T$.

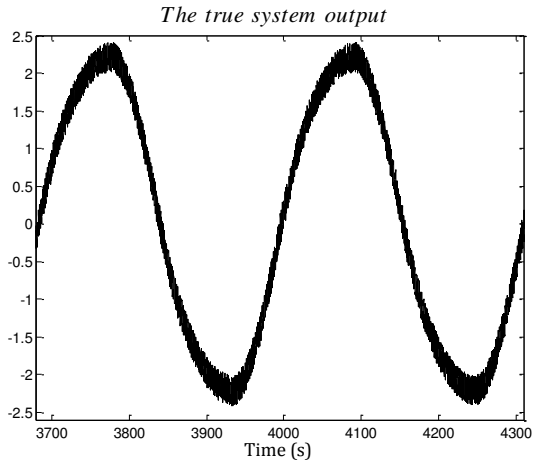

Fig. 3a. Steady-state periodic output $y_{U_1,\omega_1}(t)$ over two periods.

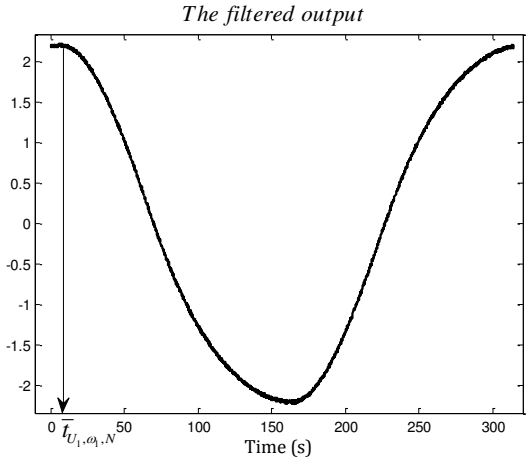

Fig. 3b. Estimated undisturbed output $\bar{y}_{U_1,\omega_1,N}(t)$ over one period.

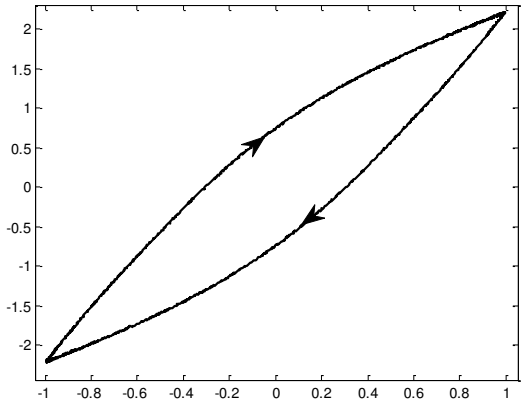

Fig. 4. Hysteresis cycle described (in steady state) by the working point ($\hat{x}_{U_1,\omega_1,N}(t)$, $\bar{y}_{U_1,\omega_1,N}(t)$)

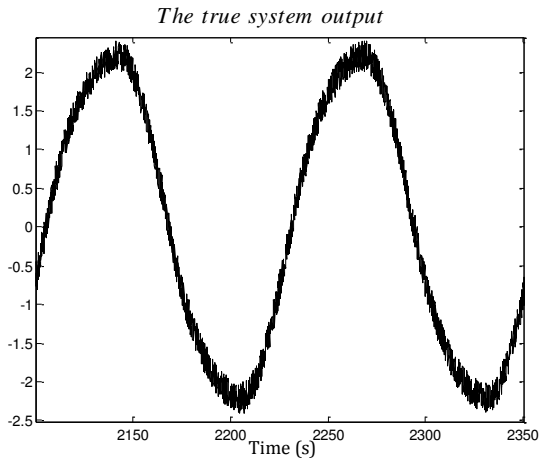

Fig. 5a. Steady-state output $y_{U_2,\omega_2}(t)$ obtained with (U_2,ω_2) over two periods.

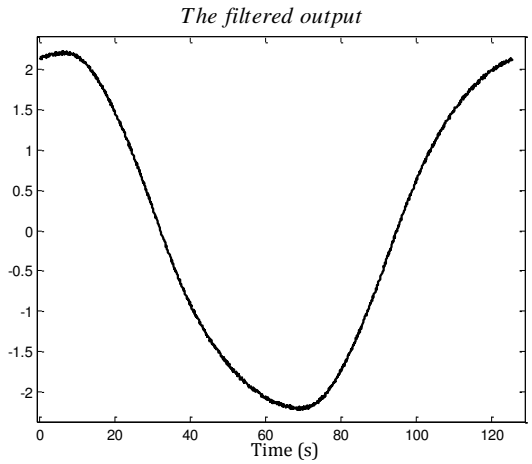

Fig. 5b. Estimated undisturbed output $\bar{y}_{U_2,\omega_2,N}(t)$ over one period.

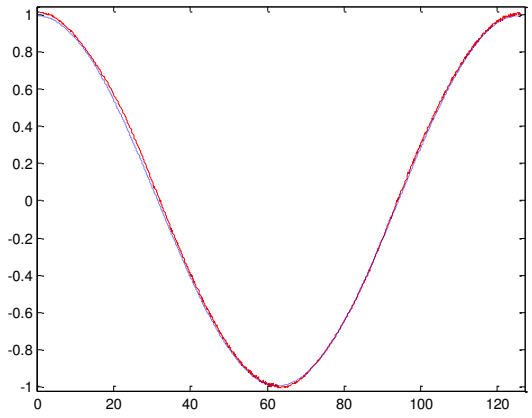

Fig. 6. Steady-state internal signal $x_{U_2,\omega_2}(t)$ (solid) and its estimate $\hat{x}_{U_2,\omega_2,N}(t)$ (dashed). The two signals are too close to be distinguished.

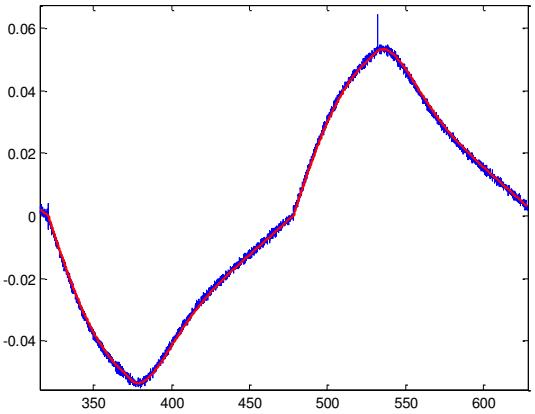

Fig. 7. Steady-state signal $w^D_{U_1,\omega_1}$ (solid) and its estimate $\hat{w}^D_{U_1,\omega_1,N}$ (dashed); the latter is also recognizable due to noise effect on it, unlike the former.

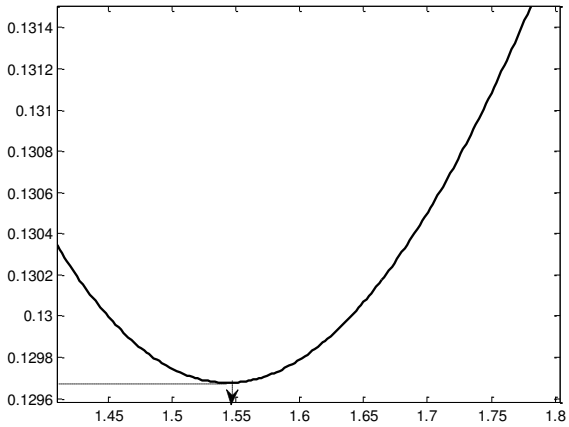

Fig. 8. Plot of $I_N(\eta)$ vs $\eta > 1$

Table IV. Frequency response estimates $\hat{G}_N(j\omega_i)$

i	1	2	3	4	5
U_i	1	1.03	1.16	1.47	3.45
$\omega_i\,(rd/s)$	0.02	0.05	0.1	0.2	0.5
$\lvert G(j\omega_i)\rvert$	1	0.96	0.88	0.66	0.26
$\lvert \hat{G}_N(j\omega_i)\rvert$	1	0.97	0.85	0.69	0.29
$\angle G(j\omega_i)$ (rd)	0.14	0.34	0.66	1.97	2.48
$\angle \hat{G}_N(j\omega_i)$ (rd)	0.15	0.32	0.68	1.94	2.45

4. CONCLUSION

The problem of system identification is addressed for Wiener systems containing nonlinear hysteretic elements. The system is represented by the model (1a-c) where the structure of $G(s)$ is not necessarily known. The proposed two-stage identification method is a combination of frequency and prediction-error techniques. It features the ability of accurately estimating the linear subsystem $G(s)$ without requiring any prior knowledge on the hysteretic operator $F[\bullet]$, except for assumption HLA. Interestingly, this assumption is satisfied by several hysteretic models. The second stage of the identification method is devoted to parameter estimation of $F[\bullet]$ on the basis of the Bouc-Wen model. It is shown that, this estimation can be accurately performed without requiring any prior knowledge on $G(s)$, except for its static gain $G(0)$. The weak coupling between the two identification stages is another feature of the developed method. To the authors' knowledge no previous study has dealt with the identification of Wiener systems involving hysteretic operators other than backlash. This study can

be continued in several directions including: (i) investigating the hysteresis parameter estimation stage (Section 4) for other hysteresis models e.g. Prandtl-Ishlinkskii model and Preisach model; (ii) investigating the possibility of developing a single stage identification scheme.

REFERENCES

Aguirre N., F. Ikhouane, J. Rodellar, R. Christenson (2012). "Parametric identification of the Dahl model for large scale MR dampers" Structural Control and Health Monitoring, vol. 19, pp. 332-347.

Bai E.W. (2003). Frequency domain identification of Wiener models. Automatica, vol. 39, pp.1521-1530.

Bai E.W. and J. Reyland (2009). Towards identification of Wiener systems with the least amount of a priori information: IIR cases. Automatica, vol. 45, no 4, pp. 956-964.

Boyd, S., L.O. Chua (1985). Fading memory and the problem of approximating nonlinear operators with Volterra series. IEEE Transactions on Circuits and Systems, CAS-32 (11), 1150–1161.

Bruls J., C.T. Chou, B.R.J. Heverkamp and M. Verhaegen (1999). Linear and nonlinear system identification using separable least squares, European Journal of Control, vol 5, pp.116-128.

Cerone V., D. Piga and D. Regrunto (2009). Parameter bounds evaluation for linear system with output backlash. IFAC Symposium on System Identification, Saint-Malo, France, pp.575-580

Crama P., and J. Schoukens (2001). Initial estimates of Wiener and Hammerstein systems using multisine excitation. IEEE Transactions on Instrum. & Measurement, vol. 50, pp. 1791-1795.

Crama P., J. Schoukens (2005). Computing an initial estimate of a Wiener–Hammerstein system with a random phase multisine excitation. IEEE Trans. Instrum. & Measur., vol. 54, pp. 117-122.

Dong, R., Tan Q., and Tan, Y. (2009). Recursive identification algorithm for dynamic systems with output backlash and its convergence. Int. J. Applied Math. Computer Science, vol. 19, pp. 631-638.

Enqvist M. (2010). Identification of block-oriented systems using the invariance property. In Giri and Bai (eds), Block-Oriented Nonlinear System Identification. Springer, pp. 149-159.

Giri F., E. Radouane, A. Brouri, F.Z. Chaoui (2014). Combined frequency-prediction error identification approach for Wiener systems with backlash and backlash-inverse operators. Automatica, Volume 50 (3), pp. 768–783.

Giri F., Y. Rochdi, A. Brouri, A. Radouane, F.Z. Chaoui (2013). Frequency identification of nonparametric Wiener systems containing backlash nonlinearities. Automatica, vol. 49, pp. 124-137.

Giri, F., Y. Rochdi and F.Z. Chaoui, (2009). An analytic geometry approach to Wiener system frequency identification, IEEE Trans. Automatic Control, vol. 54, no 4, pp. 683-696.

Gomis-Bellmunt O., F. Ikhouane, D. Montesinos-Miracle, (2009). Control of a piezoelectric actuator considering hysteresis. Journal of Sound and Vibration, vol. 326 (3), pp. 383-399.

Greblicki,W. and M. Pawlak (2008). Nonparametric System Identification. Cambridge University Press.

Hua X., Li S., Penga H. (2012). A comparative study of equivalent circuit models for Li-ion batteries. Journal of Power Sources, vol. 198, pp. 359– 367.

Hu X.L. and H.F. Chen (2008). Recursive identification for Wiener systems using Gaussian inputs. Asian Journal of Control, Vol. 10, No. 3, pp. 341 350.

Ikhouane F. and O. Gomis-Bellmunt (2008). A limit cycle approach for the parametric identification of hysteretic systems. Systems & Control Letters, vol. 57, pp 663–669.

Ikhouane F. and J. Rodellar (2007). Systems With Hysteresis: Analysis, Identification and Control using the Bouc-Wen Model. John Wiley & Sons, Sussex, UK.

Ioannou P. and J. Sun P. (1996). Robust Adaptive Control. Prentice Hall, NJ,USA.

Kuhnen K. (2003). Modeling, identification and compensation of complex hysteretic nonlinearities: a modified Prandtl-Ishlinkskii approach. European Journal of Control, vol. 9 (4), pp. 407-418.

Kiong T.K. and H. Sunan (2014). Modeling and control of precision actuators. CRC Press, Boca Raton, FL, USA.

Ljung L. (1999). System identification. Theory for the user. Prentice Hall, NJ, USA.

Lovera M., T. Gustafsson T., and M. Verhaegen (2000). Recursive subspace identification of linear and non-linear Wiener state-space models. Automatica, vol. 36, pp.1639-1650

Lyzell C., M. Andersen, and M. Enqvist (2012). A Convex Relaxation of a Dimension Reduction Problem Using the Nuclear Norm. IEEE Conference on Decision and Control, Maui, Hawaii, USA, pp. 2852-2857.

Lyzell C., M. Enqvist (2012). Inverse regression for the Wiener class of systems. IFAC symp. On System Identification, Brussels, Belgium.

Mayergoyz I. D. (2003) Mathematical Models of Hysteresis and Their Applications. Elsevier Inc.

Mzyk G. (2010). Parametric Versus Nonparametric Approach to Wiener Systems Identification. In Giri F. and E.W. Bai (2010). Block-oriented nonlinear system identification. Springer, U.K.

Pelckmans K. (2011). MINLIP for the identification of monotone Wiener systems. Automatica, vol. 47, pp. 2298–2305.

Pintelon R., P. Guillaume, Y. Rolain, J. Schoukens, and H. Van hamme (1994). Parametric Identification of Transfer Functions in the Frequency Domain-A Survey. IEEE Transactions on Automatic Control, Vol. 39 (11), pp. 2245-2260.

Radouane A., F. Giri, F. Ikhouane, F.Z. Chaoui. Wiener System Identification in Presence of Hysteresis Nonlinearities. IFAC World Congress, Cap Town, South Africa, 2014.

Reyland J., E.W. Bai (2013). Generalized Wiener system identification: General backlash nonlinearity and finite impulse response linear part. International Journal of Adaptive Control and Signal Processing, DOI: 10.1002/acs.2437.

Schoukens J., T. Dobrowiecki, and R. Pintelon, (1998). Parametric and nonparametric identification of linear systems in the presence of nonlinear distortions - a frequency domain approach. IEEE Transactions on Automatic Control, vol. 43(2), pp. 176-190.

Schoukens, M. and Y. Rolain (2012). Parametric Identification of Parallel Wiener Systems IEEE Trans. Instrum. Measurements. vol. 61, pp.2825 -2832.

Tan X. and J.S. Baras (2005). Adaptive identification and control of hysteresis in smart materials. IEEE Transactions on Automatic Control, vol. 50 (6), pp. 827-839.

Vanbeylen L. and R. Pintelon (2010). Blind maximum-likelihood Identification of Wiener and Hammerstein nonlinear block structures. In Giri & Bai (eds), Block-Oriented Nonlinear System Identification, Springer, pp. 279-298.

Vanbeylen L., R. Pintelon, and J. Schoukens (2009). Blind maximum-likelihood identification of Wiener systems. IEEE Transactions on Signal Processing, vol. 57(8), pp. 3017–3029.

Vörös J., (1997). Parameter identification of Wiener systems with discontinuous nonlinearities, Systems and Control Letters, vol. 44, pp. 363-372.

Vörös J., (2010). Compound operator decomposition and its application to Hammerstein and Wiener systems. In Giri & Bai, Block-Oriented Nonlinear System Identification, Springer, U.K.

Westwick D. and M. Verhaegen (1996). Identifying MIMO Wiener systems using subspace model identification methods. Signal Processing, 52, pp. 235–258.

Wigren T. (1993). Recursive prediction error identification using the nonlinear Wiener model. Automatica, vol. 29, pp. 1011-1025.

Wigren T. (1994). Convergence analysis of recursive identification algorithm based on the nonlinear Wiener model. IEEE Trans. Automatic Control, vol. 39, pp. 2191-2205.

Wills A. and L. Ljung, (2010). Wiener system identification using the maximum likelihood method. In Giri F. & E.W. Bai (2010). Block-oriented nonlinear system identification. Springer, U.K.

Wills A., T.B. Schön, L. Ljung, B. Ninness (2011). Blind identification of Wiener models. IFAC World Congress, Milan, Italy.

APPENDIX A. Further Information on Bouc-Wen Hysteresis Model.

Part 1. Derivation of equations (28)-(29).

Introduce the variable change $w^1(t) = k_w w(t)$, where $k_w > 0$ is any constant scalar. Then, (3a-b) rewrites in term of $w^1(t)$ as follows:

$$v(t) = \lambda_x x(t) + \lambda_w^1 w^1(t) \tag{A1}$$

$$\dot{w}^1(t) = \alpha^1 \dot{x}(t) - \beta^1 \left|\dot{x}(t)\right| \left|w^1(t)\right|^{\mu-1} w^1(t) - \gamma^1 \dot{x}(t) \left|w^1(t)\right|^{\mu} \tag{A2}$$

with $\lambda_w^1 = \lambda_w / k_w$, $\alpha^1 = \alpha k_w$, $\beta^1 = \beta / k_w^{\mu-1}$, and $\gamma^1 = \gamma / k_w^{\mu-1}$. It is readily seen that the parameters (β^1, γ^1) are still satisfying the properties $\beta^1 + \gamma^1 > 0$, $\beta^1 - \gamma^1 \geq 0$, while the parameter μ remains unchanged. That is, the couple of equations (A1)-(A2) is still defining a Bouc-Wen model, now denoted $F^1[\bullet]$, just as (3a-b) is defining $F[\bullet]$. A judicious choice of the free scalar k_w is $k_w = \lambda_w$ because this entails $\lambda_w^1 = 1$. Doing so, (A1)-(A2) boils down to (28)-(29). The latter together with (1a-c) lead to the block-diagram of Fig. A1 of the whole Wiener system.

Part 2. Additional properties of the Bouc-Wen model

In the conditions of Proposition 5, the internal state $w(t)$ of the Bouc-Wen model (28)-(29) has the following properties, where the notations are similar to those used in Assumption HLA:

a) There exist two strictly-increasing C^∞ functions W^+ and W^- such that, the steady-state signal $w(t)$ satisfies:

$$w(t) = W^+(x(t)) \text{ for all } t \in [mT\ (m+\kappa)T) \text{ and all } m \in \mathbf{N} \tag{A3}$$

$$w(t) = W^-(x(t)) \text{ for } t \in [(m+\kappa)T\ (m+1)T) \tag{A4}$$

$$W^+(x(mT)) = W^-(x(mT)) \text{ and } W^+\big(x((m+\kappa)T)\big) = W^-\big(x(m+\kappa)T)\big) \tag{A5}$$

b) The functions $W^+(.)$ and $W^-(.)$ depend on the parameters $(\alpha, \beta, \gamma, \mu)$ in equation (28) and on the excursion length $x_{\max} - x_{\min}$ of the input signal $x(t)$, but not on its period T.

c) Finally, in the case of centred inputs, i.e. when $x_{\max} = -x_{\min}$, the functions W^+ and W^- have the property, $W^-(-x) = -W^+(x)$, for all $x \in [x_{\min}, x_{\max}]$. Then, the (x, w)-hysteresis loop turns out to be symmetric with respect to the origin.

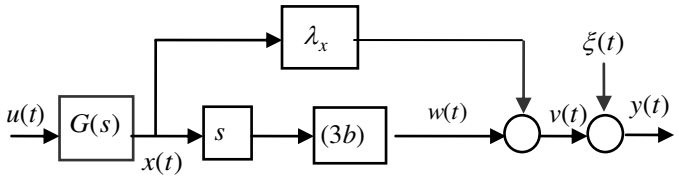

Fig. A1. Wiener System (1a-c) with $F[\bullet]$ being a Bouc-Wen hysteresis

APPENDIX B. Proof of Proposition 4.

Part 1. By (5a-b), the statement (21) implies, w.p.1, that $v(t)$ spans exactly the interval $[V_{U_1}^+(-U_1), V_{U_1}^+(U_1)]$. Since $v = F[x]$ and $x(t)$ is loading-unloading with amplitude $X_{\max}$, it follows from Assumption HLA (Part 1) that $X_{\max} = U_1$, w.p.1. By Definition 2 (Part 2), there is a unique input amplitude $U_{\max}$ such that $X_{\max}$ equals to the preceding value.

Proof of Part 2. As $x(t)$ is T-periodic, let it be represented by its Fourier series:

$$x(t) = \sum_{k=0}^{\infty} X_k \cos\left(k\omega t - \phi_k\right), \text{ with } \omega = \frac{2\pi}{T} \tag{B1}$$

The input $u(t)$ has also been represented by its Fourier series (23). Then, the relation $x = G(s)u$ entails:

$$\left|G(jk\omega)\right| = \frac{X_k}{U_k}\ , \quad \angle G(jk\omega) = \phi_k - \varsigma_k \tag{B2}$$

On the other hand, it has already been pointed out (see proof of Part 1), that the input amplitude $U_{\max}$ is selected such that (w.p.1) $x(t)$ is T-periodic loading-unloading spanning the interval $[-U_1, U_1]$. Then, it follows from Proposition 3 that the estimated signal $\hat{x}_N(t) \to x(t)$, w.p.1 as $N \to \infty$. Then, it follows comparing (B1) and (22) that, $\hat{X}_{k,N} \to X_k$ and $\hat{\phi}_{k,N} \to \phi_k$, w.p.1 as $N \to \infty$. Comparing (B2) and (25) it follows that, $\hat{G}_N(jk\omega) \to G(jk\omega)$, w.p.1 as $N \to \infty$, which proves Proposition 4 ■

APPENDIX C. **Parameter Estimation of $G(s)$ from frequency data**.

Here, the transfer function $G(s)$ is supposed to be of known structure:

$$G(s) = G(s, \theta_L) \overset{def}{=} \frac{B(s, \theta_L)}{A(s, \theta_L)} \tag{C1}$$

with,

$$A(s, \theta_L) = s^{na} + a_{na-1}s^{na-1} + \cdots + a_1 s + a_0\ ; \quad B(s, \theta_L) = b_{nb-1}s^{nb-1} + \cdots + b_1 s + b_0 \tag{C2}$$

$$\theta_L = [a_{na-1} \cdots a_1\ a_0\ b_{nb-1} \cdots b_1\ b_0]^T \in \mathbf{R}^{na+nb}, \quad (na \geq nb) \tag{C3}$$

where the degrees (na, nb) are known, but the parameter vector θ_L is not. The aim is to estimate θ_L using a given set of frequency data $G(j\omega_i)\ (i = 1 \ldots n)$. To this end, consider the following least squares estimator:

$$\hat{\theta}_{L,N} = \arg\min_{\theta} P_N(\theta) \tag{C4}$$

with

$$P_N(\theta) = \frac{1}{n}\sum_{i=1}^{n}\left|\hat{G}_N(j\omega_i)A(j\omega_i, \theta) - B(j\omega_i, \theta)\right|^2 \tag{C5}$$

where $n > na + nb$. The expression of $\hat{\theta}_{L,N}$ will be given later. First, its consistency is established.

Proposition C1. Suppose the transfer function $G(s)$ is of known structure (28a-b) and assume the polynomials $A(s, \theta_L)$ and $B(s, \theta_L)$ are coprime and $n > na + nb$. Then, the estimator (29a-b) is consistent, i.e. $\hat{\theta}_{L,N} \to \hat{\theta}_L$, w.p.1 as $N \to \infty$.

Proof. First, let us check that:

$$P_N(\theta_L) \to 0 \text{, w.p.1 as } N \to \infty . \qquad \text{(C6)}$$

Using (C1)-(C3) it follows from (C5) that:

$$P_N(\theta_L) = \frac{1}{n}\sum_{i=1}^{n}\left|\hat{G}_N(j\omega_i)A(j\omega_i,\theta_L) - B(j\omega_i,\theta_L)\right|^2$$

$$= \frac{1}{n}\sum_{i=1}^{n}\left|A(j\omega_i,\theta_L)\left(\hat{G}_N(j\omega_i) - G(j\omega_i,\theta_L)\right)\right|^2$$

which entails (C6), due to Proposition 4 which ensures that $\hat{G}_N(j\omega_i) \to G(j\omega_i,\theta_L)$, w.p.1 as $N \to \infty$. The second preliminary result is that θ_L is the only vector satisfying (C6). Specifically, the following statement holds:

$$P_N(\theta) \to 0 \text{ (w.p.1 as } N \to \infty) \text{ with } \theta \in \mathbf{R}^{na+nb} \quad \Rightarrow \quad \theta = \theta_L \qquad \text{(C7)}$$

To prove this, let us suppose that $P_N(\theta) \to 0$, w.p.1 as $N \to \infty$. Then, it follows from (C5) that, w.p.1 as $N \to \infty$, $\hat{G}_N(j\omega_i)A(j\omega_i,\theta) - B(j\omega_i,\theta) \to 0$ or, equivalently, $\hat{G}_N(j\omega_i) - G(j\omega_i,\theta) \to 0$, using (C1)-(C2). But, it has already been noticed that $\hat{G}_N(j\omega_i) \to G(j\omega_i,\theta_L)$. Then, one gets that, $G(j\omega_i,\theta) = G(j\omega_i,\theta_L)$ which, in view of (C1)-(C2), yields $B(j\omega_i,\theta)/A(j\omega_i,\theta) = B(j\omega_i,\theta_L)/A(j\omega_i,\theta_L)$ or, equivalently, $B(s,\theta)A(s,\theta_L) - B(s,\theta_L)A(s,\theta) = 0$ with $s = j\omega_i$ $(i = 1\ldots n)$. As the polynomial $B(s,\theta)A(s,\theta_L) - B(s,\theta_L)A(s,\theta)$ is of degree $na+nb$, it has at most $na+nb$ different zeros. Since the equality $B(s,\theta)A(s,\theta_L) - B(s,\theta_L)A(s,\theta) = 0$ holds for $n > na+nb$ different values of $s \in \mathbf{C}$, namely $j\omega_i$ $(i = 1\ldots n)$, it follows that the mentioned polynomial is zero. That is, one has the polynomial equality $B(s,\theta)A(s,\theta_L) = B(s,\theta_L)A(s,\theta)$, $\forall s \in \mathbf{C}$. Since $A(s,\theta_L)$ and $B(s,\theta_L)$ are coprime, the previous polynomial equality implies that $A(s,\theta_L)$ divides $A(s,\theta)$ and $B(s,\theta_L)$ divides $B(s,\theta)$. This, together with the fact that $A(s,\theta_L)$ and $A(s,\theta)$ are of the same degree and monic (higher degree coefficient equals 1), it follows that $A(s,\theta_L) = A(s,\theta)$, which also entails that $B(s,\theta_L) = B(s,\theta)$, implying that $\theta = \theta_L$. Hence, the statement (C7) is proved. The statements (C6) and (C7) show that , w.p.1 as $N \to \infty$, the function $P_N(\theta)$ possesses a global minimum equal to zero and this minimum is only achieved at $\theta = \theta_L$. It follows that, w.p.1 as $N \to \infty$, the estimator $\hat{\theta}_{L,N}$ defined by (C4)-(C5) converges to θ_L, which proves Proposition C1 ■

To complete the analysis of (C4)-(C5), its explicit solution will now be derived. To this end, introduce the notation:

$$\Psi_i^T(\omega_i) = [j\omega_i\hat{G}_N(j\omega_i)\cdots(j\omega_i)^{na}\hat{G}_N(j\omega_i) \;\; j\omega_i\cdots(j\omega_i)^{nb}]$$

Then, the cost function $P_N(\theta)$ expresses as follows:

$$P_N(\theta)=\frac{1}{n}\sum_{i=1}^{n}\left(\hat{G}_N(j\omega_i)-\Psi_i^T(\omega_i)\theta\right)\left(\overline{\hat{G}}_N(j\omega_i)-\overline{\Psi}_i^T(\omega_i)\theta\right)$$

where the bar symbol refers to complex conjugate. The estimate $\hat{\theta}_{L,N}=\arg\min_{\theta} P_N(\theta)$ is the vector θ where the derivative $dP_N(\theta)/d\theta=0$. It is easily checked that:

$$\hat{\theta}_{L,N}=\left(\sum_{i=1}^{n}\Psi_i(\omega_i)\overline{\Psi}_i^T(\omega_i)+\overline{\Psi}_i(\omega_i)\Psi_i^T(\omega_i)\right)^{-1}\left(\sum_{i=1}^{n}\Psi_i(\omega_i)\overline{\hat{G}}_N(j\omega_i)+\overline{\Psi}_i(\omega_i)\hat{G}_N(j\omega_i)\right)$$

APPENDIX D. **Proof of Proposition 6**.

Proof of Part 1. One needs to show that $J(\eta,\theta)=0\Leftrightarrow(\eta,\theta)=(\mu,\theta_H)$. For convenience, introduce the notations $\theta=[\theta_1\ \theta_2\ \theta_3]^T\in\mathbf{R}^3$ and $\theta_H=[\theta_{H,1}\ \theta_{H,2}\ \theta_{H,3}]^T\in\mathbf{R}^3$. Then, (36a) writes:

$$\dot{w}_{U_1,\omega_1}=\theta_{H,1}\dot{x}_{U_1,\omega_1}-\theta_{H,2}\left|\dot{x}_{U_1,\omega_1}\right|\left|w_{U_1,\omega_1}\right|^{\mu-1}w_{U_1,\omega_1}-\theta_{H,3}\dot{x}_{U_1,\omega_1}\left|w_{U_1,\omega_1}\right|^{\mu} \tag{D1}$$

In turn, $J(\eta,\theta)=0$ yields an equation like (D1), replacing there the $\theta_{H,i}$'s by the θ_i 's and μ by η:

$$\dot{w}_{U_1,\omega_1}=\theta_1\dot{x}_{U_1,\omega_1}-\theta_2\left|\dot{x}_{U_1,\omega_1}\right|\left|w_{U_1,\omega_1}\right|^{\eta-1}w_{U_1,\omega_1}-\theta_3\dot{x}_{U_1,\omega_1}\left|w_{U_1,\omega_1}\right|^{\eta} \tag{D2}$$

By Property (A5) (see Appendix A), the (x,w)-hysteresis loop is presently symmetrical with respect to the origin. Furthermore, by Properties (A3)-(A4), there is a sequence of time intervals, say $(t_k^-,t_k^+)\in\left[k\frac{2\pi}{\omega_1},(k+1)\frac{2\pi}{\omega_1}\right]$ $(k\in\mathbf{N})$, on which one has $w_{U_1,\omega_1}>0$, $\dot{w}_{U_1,\omega_1}>0$, and $\mathrm{sgn}(\dot{w}_{U_1,\omega_1})=\mathrm{sgn}(\dot{x}_{U_1,\omega_1})$ with $\dot{x}_{U_1,\omega_1}(t)=-U_1\omega_1\sin\left(\omega_1 t+\angle G(j\omega_1)\right)$, due to (30b). Then, (D1)-(D2) simplify to:

$$\frac{\dot{w}_{U_1,\omega_1}(t)}{U_1\omega_1\sin\left(\omega_1 t+\angle G(j\omega_1)\right)}=-\theta_{H,1}+(\theta_{H,2}+\theta_{H,3})\left(w_{U_1,\omega_1}(t)\right)^{\mu},\quad\forall t\in(t_k^-,t_k^+) \tag{D3}$$

$$\frac{\dot{w}_{U_1,\omega_1}(t)}{U_1\omega_1\sin\left(\omega_1 t+\angle G(j\omega_1)\right)}=-\theta_1+(\theta_2+\theta_3)\left(w_{U_1,\omega_1}(t)\right)^{\eta},\quad\forall t\in(t_k^-,t_k^+) \tag{D4}$$

Suppose that $\mu>\eta$ and introduce the notations:

$$z(t)=\left(w_{U_1,\omega_1}(t)\right)^{\eta},\quad\mu^*=\frac{\mu}{\eta}>1 \tag{D5}$$

Then, (D3)-(D4) imply:

$$-\theta_1+(\theta_2+\theta_3)\,z=-\theta_{H,1}+(\theta_{H,2}+\theta_{H,3})\,z^{\mu^*},\quad\forall z\in(z^-,z^+) \tag{D6}$$

where (z^-,z^+) denotes the image of (t_k^-,t_k^+) by $z(t)$. Differentiating both sides of (D6) with respect to z, yields:

$$(\theta_2+\theta_3)=\mu^*(\theta_{H,2}+\theta_{H,3})\,z^{\mu^*-1},\quad\forall z\in(z^-,z^+)$$

But, this cannot hold unless $\mu^*=1$. It turns out that $\eta=\mu$. Then, (D6) implies:

$$-\theta_1 + (\theta_2+\theta_3)\, z = -\theta_{H,1} + (\theta_{H,2}+\theta_{H,3})\, z, \quad \forall z \in (z^-, z^+)$$

In turn, this yields:

$$\theta_1 = \theta_{H,1} \text{ and } (\theta_2+\theta_3) = (\theta_{H,2}+\theta_{H,3}) \tag{D7}$$

Again, by symmetry of the (x,w)-hysteresis loop around the origin, there is a series of time intervals, say $(\tau_k^-, \tau_k^+) \in \left[k\frac{2\pi}{\omega}, (k+1)\frac{2\pi}{\omega} \right]$ $(k \in \mathbf{N})$, on which one has $w_{U_1,\omega_1} > 0$ and $\dot{w}_{U_1,\omega_1} < 0$. Then, (D1)-(D2) simplify to:

$$\frac{\dot{w}_{U_1,\omega_1}(\tau)}{U_1\omega_1 \sin\left(\omega_1\tau - \varphi(\omega_1)\right)} = -\theta_{H,1} + (\theta_{H,3}-\theta_{H,2})\,(w_{U_1,\omega_1}(\tau))^{\mu}, \quad \forall \tau \in (\tau_k^-, \tau_k^+) \tag{D8}$$

$$\frac{\dot{w}_{U_1,\omega_1}(\tau)}{U_1\omega_1 \sin\left(\omega_1\tau - \varphi(\omega_1)\right)} = -\theta_{\mathrm{H},1} + (\theta_3-\theta_2)\,(w_{U_1,\omega_1}(\tau))^{\mu}, \quad \forall \tau \in (\tau_k^-, \tau_k^+) \tag{D9}$$

where we have used the fact that $\mu = \eta$ and $\theta_{\mathrm{H},1} = \theta_1$. Comparing (D8) and (D9), gives:

$$\theta_2 - \theta_3 = \theta_{H,2} - \theta_{H,3} \tag{D10}$$

From (D7) and (D10), it follows that $\theta_2 = \theta_{H,2}$ and $\theta_3 = \theta_{3,H}$. We have thus proved that the equation $J(\nu,\theta) = 0$ has a unique solution. This proves the statement $J(\eta,\theta) = 0 \Rightarrow (\eta,\theta) = (\mu,\theta^*)$ and establishes Part 1 of Proposition 6.

Proof of Part 2. First, notice that $\Pi_{LS}(\eta)$ (defined by (39)) does exist provided the following (persistent excitation) condition holds:

$$\exists \varepsilon > 0, \forall \eta \geq 0, \forall k \geq 0 : \int_{2k\pi/\omega_1}^{2(k+1)\pi/\omega_1} \psi(\eta,t)\psi^T(\eta,t)dt > \varepsilon I_{3\times 3} \tag{D11}$$

Under this condition, $I(\eta)$ turns out to be well defined due to (41b) and (39). To prove (D11), by the contrary, consider an arbitrary sequence $\varepsilon_i > 0$, such that $\varepsilon_i \to 0$. If (D11) does not hold then, there exists a vector sequence, say $Z_i \in \mathbf{R}^3$, with unit norm ($\|Z_i\| = 1$), such that:

$$Z_i^T \left(\int_{2k\pi/\omega_1}^{2(k+1)\pi/\omega_1} \psi(\eta,t)\psi^T(\eta,t)dt \right) Z_i \leq \varepsilon_i \tag{D12}$$

for at least one k. It readily follows from (D12) that:

$$\limsup_{i\to\infty} \left(\int_{2k\pi/\omega_1}^{2(k+1)\pi/\omega_1} \left(Z_i^T \psi(\eta,t) \right)^2 dt \right) \leq 0 \tag{D13}$$

This immediately gives:

$$\limsup_{i\to\infty} Z_i^T \psi(\eta,t) = 0, \tag{D14}$$

almost everywhere on $[2k\pi/\omega_1, 2(k+1)\pi/\omega_1]$. Using (36d) and the notation $Z_i^T = [z_{i,1}\ z_{i,2}\ z_{i,3}]$, it follows from (D14) that, one has almost everywhere on $[2k\pi/\omega_1, 2(k+1)\pi/\omega_1]$:

$$z_{i,1}\, x^{D}_{U_1,\omega_1} - z_{i,2}\, D(s)[\left|\dot{x}_{U_1,\omega_1}\right| \left\| w_{U_1,\omega_1} \right|^{\mu-1} w_{U_1,\omega_1}] - z_{i,3}\, D(s)[\dot{x}_{U_1,\omega_1} \left| w_{U_1,\omega_1} \right|^{\mu}] \underset{i\to\infty}{\to} 0$$

Operating $[D(s)]^{-1}$ on the left side of the above statement yields:

$$z_{i,1}\, \dot{x}_{U_1,\omega_1} - z_{i,2} \left|\dot{x}_{U_1,\omega_1}\right| \left\| w_{U_1,\omega_1} \right|^{\mu-1} w_{U_1,\omega_1}] - z_{i,3}\, \dot{x}_{U_1,\omega_1} \left| w_{U_1,\omega_1} \right|^{\mu} + \delta \underset{i\to\infty}{\to} 0 \qquad \text{(D15)}$$

with δ an exponentially vanishing term. Consider the time subintervals $(t_k^-, t_k^+) \in \left[k\frac{2\pi}{\omega_1}, (k+1)\frac{2\pi}{\omega_1} \right]$ $(k \in \mathbf{N})$, already introduced in Part 1. On these subintervals, one has $w_{U_1,\omega_1} > 0$, $\dot{w}_{U_1,\omega_1} > 0$ and $\dot{x}_{U_1,\omega_1}(t) > 0$. It follows that (D15) simplifies, almost everywhere on the above subintervals, to:

$$-z_{i,1} + (z_{i,2} + z_{i,3}) \left| w_{U_1,\omega_1} \right|^{\eta} \underset{i\to\infty}{\to} 0 \qquad \text{(D16)}$$

Then, the time-varying (loading-unloading) nature of w_{U_1,ω_1} yields:

$$\lim_{i\to\infty} z_{i,1} = \lim_{i\to\infty} (z_{i,2} + z_{i,3}) = 0 \qquad \text{(D17)}$$

Similarly, considering the subinterval $(\tau_k^-, \tau_k^+) \in \left[k\frac{2\pi}{\omega_1}, (k+1)\frac{2\pi}{\omega_1} \right]$, introduced in Part 1 of this appendix, it follows that (D15) simplifies (almost everywhere) on this interval to:

$$-z_{i,1} + (z_{i,2} - z_{i,3}) \left| w_{U_1,\omega_1} \right|^{\eta} \underset{i\to\infty}{\to} 0 \qquad \text{(D18)}$$

Again, using the loading-unloading nature of w_{U_1,ω_1}, one gets:

$$\lim_{i\to\infty} z_{i,1} = \lim_{i\to\infty} (z_{i,2} - z_{i,3}) = 0 \qquad \text{(D19)}$$

It follows from (D17) and (D19) that all three components $(z_{i,1},, z_{i,2}, z_{i,3})$ converge to zero as $i \to \infty$. But this contradicts the fact that $\left\| Z_i \right\| = 1$. Hence, (D11) holds.

Now, to prove the result of Proposition 6 (Part 2), recall that from (41b) one has $I(\eta) = J(\eta, \Pi_{LS}(\eta))$. This implies that $I(\mu) = J(\mu, \Pi_{LS}(\mu)) = J(\mu, \theta_H)$ (using (40)). As $J(\mu, \theta_H) = 0$, one gets that $I(\mu) = 0$. The question is whether this global minimum is unique. Suppose that there exists a second global minimum at η i.e. $I(\eta) = 0$. This implies that $J(\eta, \Pi_{LS}(\eta)) = 0$ which, in view of Part 1 of this proposition, gives $(\eta, \Pi_{LS}(\eta)) = (\mu, \theta^*)$. This proves the uniqueness of the global minimum of the function $I(\eta)$ and completes the proof of Proposition 5 ■